Title page

Late Devonian felsic magmatism in southern New Brunswick and its association with a large igneous province that may have contributed to the Frasnian-Famennian extinction

Jaroslav Dostal[1*], Pierre Jutras[1], Luigi A. Solari[2]

[1] *Department of Geology, Saint Mary's University, Halifax, Nova Scotia B3H, Canada*

[2] *Instituto de Geología, Universidad Nacional Autónoma de México, 04510 Mexico City, Mexico*

---

[*] Corresponding author.

E-mail address: jdostal@smu.ca (J. Dostal)

Felsic rocks of the Piskahegan Group and coeval plutons form a major part of a Late Paleozoic epicontinental caldera in southwestern New Brunswick, Canada. The caldera forms an elliptical structure with a length of ~34 km and a width of ~13 km. It hosts a significant polymetallic deposit of tin, molybdenum, indium and bismuth associated with mid-sequence granitic intrusions. The caldera formed in the aftermath of the late Early to Middle Devonian Acadian Orogeny during the opening of the late Paleozoic Maritimes Basin in the Northern Appalachian Belt. Its surrounding successions are largely composed of bimodal igneous rocks that were derived from two distinct sources: upper mantle-derived mafic magma and lower crust-derived felsic magma. The rocks that marked the beginning of volcanic activity in the caldera are no younger than 374.2±2 Ma, whereas the uppermost dated volcanic unit in the complex yielded an age of 364.6±0.7 Ma. The latter is conformably overlain by a succession of red beds and undated basalts that also overlie penecontemporaneous felsic volcanic rocks adjacent to the caldera. The post-orogenic felsic rocks are fractionated, peraluminous A-2 type rocks with silica contents ranging from ~70 to ~79 wt.% along with high K_2O contents and $\varepsilon_{Nd}(t)$ ranging from -0.10 to +1.05. They were generated by the melting of lower crustal basement rocks linked to a lithospheric plate that was metasomatized during the Neoproterozoic. Based on available geochemical, geophysical and structural data on Late Paleozoic rocks of southeastern Canada, the melting may have been triggered by the injection of profuse mafic magma that eventually formed a thick underplating at the base of the crust in association with heat derived from an underlying mantle plume and conveyed by transtensional structures. Basal rocks of the Piskahegan Group (the Intracaldera Sequence) and penecontemporaneous volcanic rocks in Nova Scotia are interpreted as small erosional remnants of a Large Igneous Province (LIP) based on the extensive exposure of large coeval plutons throughout southeastern Canada. The new

geochronological data suggests that profuse late Frasnian magmatism in this LIP could have contributed to the environmental deterioration that led to a significant extinction at the Frasnian-Famennian boundary (the Kellwasser Event).

1. Introduction

The origin of voluminous rhyolitic rocks from compositionally bimodal suites has been extensively discussed and resulted in a century-long debate (e.g., Bowen 1928; Marsh, 2006). Long-standing questions that remain revolve around how felsic magmas are generated in these bimodal suites, and to what extent felsic magmas can evolve by protracted fractional crystallization in crustal subvolcanic magma chambers. The question is important for understanding the origin and evolution of the continental crust (e.g., McBirney, 2006). Comprehension of crustal silicic magmatism requires an investigation of both plutonic and volcanic rocks (e.g., Keller et al., 2015; Lundstrom and Glazner, 2016). Thus, volcanic rocks associated with coeval, shallow-seated plutonic complexes offer the opportunity to correlate contemporaneous processes and events in the volcanic and plutonic records, which can help clarify relationships between plutons and volcanic rocks as well as improve our understanding on the origin and evolution of highly silicic magma systems. In this paper, we investigate Upper Devonian felsic volcanic rocks and coeval plutons from the Mount Pleasant caldera and its surroundings in southwestern New Brunswick, Canada. The caldera is associated with a significant polymetallic deposit of tungsten-molybdenum-bismuth with tin-indium zones (Thorne et al., 2013; Mohammadi et al., 2020a). In addition, earlier studies have established that the end of the Devonian was a major period of magmatism in the northern Appalachians, although its record is largely dominated by intrusive rocks (Kellet et al., 2014). Thus, the geochemistry and geochronology of volcanic rocks and coeval plutons in the Mount Pleasant area can provide key insights into the geodynamic evolution of the magmatic system.

Mafic and intermediate volcanic rocks in and around the caldera were investigated by Dostal and Jutras (2016), whereas spatially and temporally associated granitic intrusions were studied by Yang et al. (2003). The purpose of this study is to (a) provide geochemical and isotopic data from felsic volcanic rocks of the Piskahegan Group and relate them to associated granites in the caldera; (b) report the first U-Pb zircon ages of volcanic units within the caldera; and (c) constrain the origin of these intrusive and extrusive felsic rocks in the context of caldera evolution as well as that of the magmatic system as a whole.

2. **Geological setting**

The Mount Pleasant caldera complex in southwestern New Brunswick is underlain by basement rocks of the South Ganderian domain (*sensu* Jutras and Dostal, 2023) of the northern Appalachian Belt, which is one of many exotic lithospheric blocks that broke away from the supercontinent Gondwana during the Early Ordovician and eventually accreted to composite Laurentia (the North American craton) in Late Ordovician to late Early Devonian times (Jutras and Dostal, 2023, and references therein). The caldera complex is located at the southwestern margin of the Maritimes Basin (Fig. 1A), a large (~140,000 km^2) composite basin comprised of uppermost Middle Devonian to Lower Permian sedimentary and volcanic rocks. This successor basin was initiated after the late Early to early Middle Devonian Acadian Orogeny (~405-390 Ma; Gibling et al., 2019, and references therein). The basin opened by pull-apart transtension concentrated along large E-W trending dextral fault systems that accommodated the migration of compressional stresses from southeastern Canada to New England in late Middle to Late Devonian times (Jutras and Dostal, 2019). This transition from orogenic compression to transtension was rapid (Dostal et al., 2006), and it generated numerous occurrences of late Middle Devonian to Early Carboniferous plutonic and volcanic complexes throughout southeastern Canada, in New Brunswick, Nova Scotia, Newfoundland and eastern Quebec. The intrusive components are found throughout that area (e.g. Kellet et al., 2014; 2021), but the Devonian volcanic components are mostly exposed along the southern margin of the Maritimes Basin in Cape Breton Island, northern mainland Nova Scotia and southern New Brunswick (e.g., Dunning et al., 2002; Keppie et al., 1997), whereas Lower Carboniferous volcanic rocks occur in more central parts of the basin (e.g., Barr et al., 1985, LaFlèche et al., 1998; Jutras et al., 2018; Jutras and Dostal, 2019). In addition to granitic plutons (including the large South Mountain Batholith), the intrusive components in mainland Nova Scotia are also characterized by numerous mafic/lamprophyric dykes bordering a large E-W Late Devonian fault system (Ruffman and Greenough, 1990).

Magmatic activity in and around the Maritimes Basin is related to several stages of post-Acadian pull-apart transtension. One of the most important manifestations of this magmatism is the Upper Devonian Piskahegan Group of southwestern New Brunswick, which includes rhyolites and subordinate mafic flows, tuffs, ignimbrites and sedimentary rocks that occupy and border the Mount Pleasant caldera complex along with some coeval granites (McCutcheon et al. 1997). The caldera complex is a NNE-trending elliptical structure that is about 34 km long and 13 km wide, as outlined by magnetic and regional gravity surveys (McLeod and Smith, 2010). However, the northern half is covered by Carboniferous sedimentary and volcanic rocks, thus reducing the exposed length of the caldera complex to ~15 km (Fig. 1B). Large rock-fall boulders of rhyolite dated at 368.7 ± 1.3 Ma near the base of a succession of late Visean conglomerates in more central parts of the Maritimes Basin at Hardwood Ridge (Fig. 1A) are interpreted as forming the local pre-Carboniferous basement rocks (Jutras et al., 2018) and suggest that volcanic rocks of the Piskahegan Group extend well beyond the caldera itself, buried beneath thick Carboniferous strata.

The caldera complex overlies Ordovician and Silurian turbiditic metasedimentary rocks of the Ganderian domain, whereas Late Silurian to Late Devonian granitic rocks of the Saint George Batholith border the caldera complex along its southern margin. The polymetallic deposit includes ~33 Mt of ore with 0.21% W, 0.1% Mo, 0.08 % Bi, and ~4.8 Mt of ore with 0.82% Sn and 129 ppm In, which makes it the largest known resource of indium (Sinclair et al., 2006). The deposit crops out near the southwestern margin of the caldera complex and is mainly comprised of mineralized stockworks and quartz veinlets hosted by high-level granitic rocks. Mineralization was associated with caldera collapse and resurgent doming in response to degassing of the magma chamber (Thorne et al., 2013).

3. Stratigraphy and petrography of the Piskahegan Group

McCutcheon et al. (1997) subdivided the group into time equivalent Intracaldera and Exocaldera sequences, which are still poorly correlated with each other (Thorne et al., 2013). McCutcheon et al. (1997) also included a younger Late Caldera-Fill Sequence (Fig. 1C), which is interpreted as the product of a second-generation caldera (Thorne et al., 2013). The latter authors note that the uppermost part of the Late Caldera-Fill Sequence (the Kleef Formation) onlaps the Exocaldera Sequence, suggesting that the two successions are in part coeval, which is supported by our new geochronological data (subsequent section). All three sequences include mafic and felsic volcanic rocks intercalated with sedimentary rocks, but only the lower part of the Exocaldera and Intracaldera sequences include intermediate volcanic rocks.

The Piskahegan Group has been correlated with volcanic rocks of the Upper Devonian Harvey Group (Dostal et al., 2016; Dostal and Jutras, 2016), which is exposed ~30 km northwest of the Mount Pleasant caldera complex (Fig. 1A). Aeromagnetic and gravity data (e.g., McLeod and Smith, 2010) suggest that the Piskahegan and Harvey groups connect beneath younger, Carboniferous rocks. Moreover, Upper Devonian red beds, basalts and rhyolites in northern mainland Nova Scotia and Cape Breton Island (the Fountain Lake Group as well as the McAras Brook and Fisset Brook formations) are also considered to be at least in part equivalent to the Harvey and Piskahegan groups of New Brunswick (Gibling et al., 2019, and references therein).

3.1. The Intracaldera Sequence

The Intracaldera Sequence consists in ascending stratigraphic order of the Scoullar Mountain, Little Mount Pleasant and Seelys formations (Fig. 1C). In addition, the Intracaldera Sequence is intruded by granitic bodies of the McDougall Brook and Mount Pleasant granitic suites (Yang et al., 2003; Thorne et al., 2013).

The Scoullar Mountain Formation crops out near the periphery of the caldera complex at the contact with pre-caldera rocks (Fig. 1B). The formation is up to 450 m thick and contains both sedimentary and volcanic rocks (McCutcheon et al., 1997). In addition to mafic and intermediate volcanic rocks (Dostal and Jutras, 2016), it hosts subordinate felsic volcanic rocks, including quartz-feldspar crystal tuffs and rhyolites.

The overlying Little Mount Pleasant Formation is exposed in the southern part of the caldera complex (Fig. 1B). McCutcheon et al. (1997) suggested a thickness of up to 700 m for this unit, which is composed of flow-banded rhyolite as well as quartz-feldspar crystal tuff that contains various pumice fragments of porphyritic rhyolitic material. Phenocrysts constitute about 25-40 % of the rhyolite and include plagioclase (oligoclase), K-feldspar and quartz (Anderson, 1992).

The disconformably overlying Seelys Formation is up to 500 m thick (McCutcheon et al. (1997) and is composed of pyroclastic rhyolitic flow deposits (Anderson, 1992) that contain various volcaniclastic rocks ranging from lithic and lithic lapilli tuffs to crystal tuffs, as well as strongly welded crystal tuffs. Plagioclase, K-feldspar and quartz phenocrysts are typically 2-4 mm in size and constitute about 15-20% of the rock. Anderson (1992) reported rare biotite, but the rocks otherwise lack mafic minerals.

3.2. The intracaldera granites and overlying Late Caldera-Fill Sequence

The Mount Pleasant Intracaldera Sequence is intruded by the McDougall Brook and Mount Pleasant granitic suites. Based on Re-Os dates on mineralization events associated with the latest granitic intrusions in the southern part of the caldera, Thorne et al. (2013) determined that granites in that sector are likely no younger than 370±2 Ma. Granitic bodies of the McDougall Brook suite in the northern part of the caldera are unconformably overlain by the Big Scott Mountain and Kleef formations of the Late Caldera-Fill Sequence and, although undated, are assumed to be more-or-less coeval with petrographically similar granites of the same suite to the south (McCutcheon et al., 1997), which have an upper limit of 370±2 Ma (Thorne et al., 2013). The intrusions are mainly composed of porphyritic monzogranite containing phenocrysts of plagioclase, K-feldspar and quartz (Yang et al., 2003). The Big Scott Mountain Formation is comprised chiefly of flow-banded rhyolites and lithic or crystal tuffs, whereas the Kleef Formation includes mainly red-beds and continental tholeiites (Dostal and Jutras, 2016). The rhyolites are porphyritic, with phenocrysts of plagioclase, K-feldspar and quartz set in a fine-grained matrix of the same minerals (McCutcheon et al., 1997). Sections of the Big Scott Mountain and Kleef formations are unconformably truncated by late Visean red beds of the Percé Group (*sensu* Jutras et al, 2018) and are therefore incomplete. McCutcheon et al. (1997) estimated a minimum thickness of up to ~ 175 m for the Big Scott Mountain Formation and of ~160 m for the Kleef Formation.

3.3. The Exocaldera Sequence

In ascending order, the Exocaldera Sequence includes the Hoyt Station Basalt (~20 m), rhyolites and tuffs of the Rothea Formation (~72 m), and basaltic and andesitic lava flows of the South Oromocto Andesite (~130 m), which are altogether thought to be coeval with rocks of the Intracaldera Sequence (McCutcheon et al., 1997). The sequence also includes red beds, tuffs and basalts of the Carrow Formation (~315 m) as well as felsic rocks of the overlying Bailey Rock Rhyolite (~30 m), which these authors interpreted as younger than the Intracaldera Sequence, but entirely older than the Late Caldera-Fill.

The mainly sedimentary Carrow Formation hosts fossils that are characteristic of the uppermost Devonian (McGregor and McCutcheon, 1988), and Tucker et al. (1998) subsequently obtained a U-Pb zircon age of 363.8 ± 2.2 Ma from tuff near the base of this unit, as well as a U-

Pb zircon age of 363.4 ± 1.8 Ma in the overlying Bailey Rock Rhyolite. The latter is particularly well exposed along the northern margin of the caldera complex and is characterized by phenocrysts of feldspars and quartz set in a mostly recrystallized and in part devitrified groundmass. Flow-banding textures are also present. Feldspars are usually altered, although some fresh albitic plagioclase and K-feldspar relicts are preserved.

4. Analytical methods

Whole-rock major and trace elements (Table 1) were determined using lithium metaborate–tetraborate fusion at Activation Laboratories Ltd. in Ancaster, Ontario, Canada. Major elements were analyzed by an inductively coupled plasma-optical emission spectrometer, whereas trace elements were determined by an inductively coupled plasma-mass spectrometer (ICP-MS). Replicate analyses of the reference standard rocks indicate that the 1-sigma errors are between 2% and 10% of the values cited (excluding some trace element data, which are close to their detection limit). Further information on major and trace element analyses from Activation Laboratories are available at www.actlabs.com.

The Sr–Nd isotopic compositions of three samples (Table 2) were determined using a Triton Plus thermal ionization mass spectrometer (Thermo) at the Institute of Geology of the Czech Academy of Sciences, Prague (Czech Republic), following the methods described by Ackerman et al. (2020). The external reproducibility of the analyses was monitored through the long-term analyses of NIST SRM 987 (Sr) and JNdi-1 (Nd) solutions, which yielded $^{87}Sr/^{86}Sr$ of 0.710249 ± 5 (2σ, n = 44) and $^{143}Nd/^{144}Nd$ of 0.512099 ± 6 (2σ, n = 26), respectively. The five other samples selected for the isotope determinations were analyzed by isotope dilution at the

Atlantic Universities Regional Facility at the Department of Earth Sciences of Memorial University of Newfoundland (St. John's, Newfoundland, Canada). The Nd and Sr isotopic ratios were determined using a multicollector Finnigan MAT 262 thermal ionization mass spectrometer. Replicate analyses of the LaJolla standard that were determined during the run yielded an average ^{143}Nd/^{144}Nd value of 0.511849±9 (2σ), whereas replicate runs for the NBS 987 Sr standard gave an average ^{87}Sr/^{86}Sr value of 0.710250±11 (2σ). More information on these procedures is available in Pollock et al. (2015).

Two samples were selected for U-Pb zircon age dating (NB07-66 from rhyolite of the Scoullar Mountain Formation, and NB07-32 from rhyolite of the Big Scott Mountain Formation). Heavy minerals were separated from these samples using standard techniques (e.g., Solari et al., 2007). For each sample, about 50 zircon crystals were mounted in epoxy resin and polished to expose their internal structure in order to select the sites for U-Pb analyses. The selected zircon grains were prismatic with well-defined bi-pyramidal terminations and with length/width ratios of up to 4:1. Cathodoluminescence (CD) imaging was used to observe internal structures in order to help choose the sites for analysis and help with interpreting the U-Pb results.

U-Pb isotope and trace element contents in zircons were measured by laser ablation ICP-MS at the Laboratorio de Estudios Isotópicos, Centro de Geociencias, Universidad Nacional Autónoma de Mexico, using a Thermo ICap Qc quadrupole coupled with a Resolution M050, 193 nm excimer laser ablation workstation. Following the analytical procedures described by Solari et al. (2018), a 23 µm spot was employed, with a repetition rate of 5 Hz and a fluence of 6 J/cm-2. The standard zircon 91500 (1065.4±0.6 Ma, TIMS age, Wiedenbeck et al., 1995) was employed as the primary standard. Additionally, the Plešovice standard zircon (337.13±0.37 Ma, TIMS age, Sláma et al., 2008) was employed as the control standard, which, during the current analytical session, yielded an age of 335.1±2.9 Ma (n=9, MSWD= 2.1). Once the long-term variance calculated on external standards is added (e.g., Sliwinski et al., 2022), the obtained age and uncertainty agree with its accepted age. Data processing was performed offline using the Iolite software v. 4.5 (Paton et al., 2010) and the Vizual Age data reduction scheme of Petrus and Kamber (2012). Because the non-radiogenic ^{204}Pb signal is swamped by the ^{204}Hg isobar, no common Pb correction was applied. Data were exported from Iolite and mean ages from the concordia diagrams were calculated using IsoplotR (Veermesch, 2018). The calculated age uncertainties are reported at a 2-sigma level.

For the purpose of deriving crystallization temperatures, zircon trace element concentrations were acquired from the same spots as those from which the zircon U-Pb data were obtained. The NIST 610 glass was used as an external standard for recalculating zircon trace element concentrations, employing ^{29}Si as an internal standard isotope while assuming a stoichiometric value of 15.323 mol. The analytical data for zircon isotopes and trace elements are reported as a Supplementary Electronic Material file.

5. Results

5.1. *Geochronology*

In rhyolite sample NB07-32 from the Big Scott Mountain Formation, 29 out of 35 zircon analyses were retained as they had a discordance of less than 10%. However, four of these selected grains were further excluded (uncolored ellipses in Fig. 2) because they are not concordant, either due to Pb loss or convoluted dated areas containing a mixture of inherited domains. The remaining 25 zircon crystals are prismatic and euhedral to subhedral in shape, with Th/U ratios higher than 0.1. They are colorless to light brown, and, in cathodoluminescence, are characterized by concentric oscillatory zoning. These characteristics indicate their magmatic origin, which makes them suitable for the determination of crystallization age. These zircon crystals yielded a concordant age of 365.0±1.8 Ma, which is interpreted as the age of crystallization of the sample.

Thirty-five zircon crystals from sample NB07-66 (rhyolite of the Scoullar Mountain Formation) were analyzed. Twenty-six of these analyses were considered meaningful and acceptable with a discordance of less than 10% or without convoluted textures in CD images. Zircon grains were mostly colourless and transparent, prismatic, and subhedral to euhedral. They showed oscillatory zoning and had Th/U ratios higher than 0.1, which indicate an igneous origin (Corfu et al., 2003). One of the zircon grains (pink ellipse in Fig. 2) with a concordant age of ca. 600 Ma is interpreted as inherited from the late Neoproterozoic basement that underlies a large part of the Ganderian domain (e.g. van Staal et al., 2009). This analysis was therefore not included in the set used for the calculation of crystallization age. The remaining 25 analyses yielded a concordant age of 374.2±2 Ma, which is interpreted as the crystallization age of this sample.

5.2. Whole-rock geochemistry

Felsic rocks from different stratigraphic intervals of the Piskahegan Group are geochemically quite similar. Apart from some lower SiO_2 contents in some areas of the suite, the

McDougall Brook granites are also compositionally quite similar to felsic volcanic rocks of the Piskahegan Group that both preceded and followed the intrusions (Figs. 3-6). All the felsic rock units show high K_2O contents (Fig. 3A), plotting within the high-K calc-alkaline and shoshonitic ranges of Peccerillo and Taylor (1976). However, their Na_2O contents are quite low, which brings them outside the alkalic range of Frost et al. (2001). The uniformity of Na_2O contents, which do not vary significantly with increasing LOI values (Table 1), suggests that their low contents are not solely an artifact of alteration. The Piskahegan Group rhyolites and coeval granites are also peraluminous and mostly ferroan in composition (Fig. 3C-D).

The Piskahegan Group rhyolites and associated granites have low contents of CaO, FeO_t, MgO, TiO_2 and P_2O_5 (Table 1), which is typical of A-type felsic magmas (King et al. 1997). Their high contents of high-field strength elements (HFSEs) are also typical of A-type felsic magmas (Fig. 4A), and their relative contents in Ce, Y and Nb more specifically indicate an A2-type affinity (Fig. 4B), which suggests a crustal source (Eby, 1992). Furthermore, their trace element contents best suggest a post-orogenic setting (Fig. 4C; after Pearce, 1996), which is consistent with their emplacement in the aftermath of the Acadian Orogeny.

Based on chondrite-normalized REE plots (Fig. 5), the Piskahegan Group rhyolites and coeval granites are all similarly enriched in light rare earth elements (LREE) and bear strongly negative Eu anomalies. In a primitive mantle-normalized diagram with elements arranged in order of decreasing incompatibility from left to right, all rocks show pronounced negative Nb-Ta anomalies (Fig. 6). This is interpreted as inheritance from a long history of subduction beneath Ganderian domains preceding the Acadian Orogeny, which was the culmination of multiple oceanic plate closures that formed the Canadian Appalachian belt (Jutras and Dostal, 2023, and references therein). In contrast, the rocks show enrichments in some large ion lithophile elements, including Rb, Cs, Th, U, K and Pb, but relative depletion in Ba, Sr, P, Eu and Ti, which are characteristics of highly fractionated rhyolites and granites derived from lithospheric/crustal sources. Plotting of Rb/Sr against Sr (Fig. 7A) confirms that plagioclase fractionation played a significant role during the evolution of the felsic magma. The plot also shows that the basal succession in the caldera (the Scoullar Mountain, Little Mount Pleasant and Seelys formations) are more fractionated than the subsequent McDougall Brook granites and younger volcanic units (the Big Scott Mountain Formation and Bailey Rock Rhyolite).

The Scoullar Mountain Formation shows a distinctly bimodal succession and is characterized by basalts and andesites separated by a large silica gap from highly silicic rhyolites (Dostal and Jutras, 2016). Plotting of Th/Yb against SiO_2 shows that mafic-to-intermediate and felsic rocks of the Scoullar Mountain Formation are not related by fractional crystallization (Fig. 7B).

5. 3. Neodymium isotopes

Whole-rock Nd isotopic data from felsic rocks of the Piskahegan Group and the mid-succession McDougall Brook Granitic Suite are given in Table 2 and plotted in Figure 8. Their calculated initial $\varepsilon_{Nd}(t)$ values range from + 0.33 to + 0.95 (Table 2) and approximate the values of chondrites, suggesting that the rocks were derived from a source with a long-term history of near chondritic Sm-Nd values. These values are similar to the - 0.10 to + 1.06 range obtained by other authors from the same units (Anderson, 1992; Whalen et al., 1996) as well as from the adjacent Mount Douglas Granite (Mohammadi et al., 2020b; dated at 368±1 Ma by Mohammadi et al., 2020a), which are also plotted in Figure 8. The $\varepsilon_{Nd}(t)$ values are also relatively similar to those obtained from mafic and intermediate rocks of the Piskahegan Group (Dostal and Jutras, 2016), although a trend of decreasing $\varepsilon_{Nd}(t)$ values from mafic to felsic rocks is clearly observed . Moreover, $\varepsilon_{Nd}(t)$ values from the Piskahegan Group and associated granites are well within the range of values from other volcanic rocks that were emplaced on Ganderian crust in late Silurian to Early Devonian times in New Brunswick (Dostal et al., 2016, 2021, 2022) as well as the range of values from igneous rocks of various ages in the adjacent Avalonian domain (e.g., Whalen et al., 1996; Keppie et al., 1997, Pe-Piper and Piper, 1998; Papoutsa et al., 2016), which all fit within the Avalonian envelope of Murphy et al. (2008).

Based on DePaolo (1988), neodymium depleted-mantle model ages for rocks of the Piskahegan Group range from 800 to 1,100 Ma (Table 2). It is noteworthy that, again, these values are similar to those reported for Silurian to Carboniferous igneous rocks in the Maritimes Basin in Ganderian and Avalonian crust (Keppie et al., 1997; Pe-Piper and Piper, 1998). These similarities imply that the values represent a bulk-weighted average of a similar source, which is consistent with the inferred similarities in the Neoproterozoic histories of the Avalonian and Ganderian domains as peri-Gondwanan active margins (e.g., van Staal et al., 2012).

5.4. Saturation and crystallization temperatures

The saturation temperature of some accessory minerals, namely zircon, monazite and apatite, can be used to characterize the thermal history of an igneous rock and help assess its petrogenesis. In particular, zircon saturation temperatures (T_{Zr}) have been utilized to classify granites as either "hot" or "cold", with respectively T_{Zr} >800^{o}C and T_{Zr} < 800^{o}C (e.g., Miller et al., 2003). "Hot" granites are typically assumed to be generated in an anhydrous setting by crustal melting or by the fractionation of mantle melts (with or without crustal contamination), and subsequently transported in a crystal-poor state (Miller et al., 2003; Azadbakht et al., 2019). “Cold” granites are thought to be calc-alkaline felsic magmas typically generated by water-fluxed crustal melting at lower temperatures (Miller et al., 2003). The same applies to felsic volcanic rocks.

We have calculated the zircon, monazite and apatite saturation temperatures of rhyolite samples from all five formations of the Piskahegan Group that include felsic units, as well as granite samples from the McDougall suite (Table 3). Based on the trace element contents of zircons from the two dated samples (Supplementary Electronic Material), we also used the Ti-in-zircon thermometer ($T_{Ti\text{-}in\text{-}zircon}$) for rhyolites of the Scoullar Mountain and Big Scott formations by following the procedure of Ferry and Watson (2007). Zircon saturation temperatures (T_{Zr}) were calculated in accordance with Watson and Harrison (1983), whereas monazite saturation temperatures were calculated in accordance with Montel (1993) by relating the concentrations of LREE to the bulk composition of the magma. In addition, apatite saturation temperatures were calculated in accordance with Harrison and Watson (1984).

Comparable saturation temperatures >800^{o}C were obtained for all units with all four calculations (Table 3). Although a $T_{Ti\text{-}in\text{-}zircon}$ of 769±39^{o}C was obtained for the Scoullar Mountain rhyolite (NB07-66), Schiller and Finger (2019) proposed a significant upward correction for such temperature estimates. These similarly high saturation and crystallization temperatures suggest that the felsic melts were “hot” and that they were generated by an influx of heat from mafic magma injections rather than by an influx of aqueous fluids (Miller et al., 2003; Azadbakht et al., 2019). The results also imply that the different rhyolites and granites have a similar thermal history.

6. Discussion

6.1. Alteration

Rocks of the Piskahegan Group are in part modified by secondary processes. In some samples, the concentration of mobile elements, such as K_2O and Na_2O, shows some scattering in various element ratio diagrams, suggesting minor mobility of these elements. These samples were eliminated from our data, which only include samples with lost-on-ignition (LOI) values <4%. The remaining samples show coherent profiles in chondrite-normalized REE diagrams and primitive mantle-normalized plots, suggesting that most major and trace elements retained their original magmatic concentrations. This also applies to the Nd-isotopic characteristics of the rocks. However, high Rb/Sr ratios of either primary magmatic or secondary (alteration) origin in most analyzed rocks led to a large error range of calculated $^{87}Sr/^{86}Sr$ ratios (e.g., Jahn et al., 2001). Thus, Sr isotopic values are not included in Table 2 and are not further considered.

6.2. Petrogenesis

Felsic rocks of the Piskahegan Group and coeval granites are K-rich (Fig 3A-B), peraluminous (Fig. 3C), mostly ferroan (Fig. 3D), and have trace element contents typical of A2-type felsic rocks (Figs. 4A-B). Their trace element compositions suggest a post-orogenic setting (Fig. 4C), which is consistent with their occurrence in the aftermath of the Acadian Orogeny and in association with the development of post-orogenic successor basins. However, these basinfills are not simple post-orogenic molasse, but the products of transtensional tectonics that regionally developed in synchronicity with post-orogenic rebound when compressional stresses migrated from southeastern Canada to New-England near the Middle to Late Devonian boundary (Jutras and Dostal, 2019), which is consistent with the within-plate, A2-type compositions of felsic rocks of the Piskahegan Group.

Several petrogenetic models have been proposed for the origin of peraluminous A-type granites and rhyolites. They include: (1) significant fractional crystallization of mantle-derived basaltic magma (e.g. Namur et al., 2011), (2) mixing of mantle-derived melts with crustal material (e.g., Narshimha and Kumar, 2023), and (3) partial melting of crustal rocks triggered by underplated mafic magma (e.g., Bonin, 2007). In the case of felsic rocks from the Piskahegan Group and associated granites, high Ce paired with low Nb/Y (Fig. 4B) argue against their origin by extensive fractional crystallization of mantle-derived mafic magma (Eby, 1992). In addition, unrelated Th/Yb ratios do not suggest that felsic rocks of the Scoullar Mountain Formation are fractional crystallization products of their associated basalts and andesites (Fig. 7B). Furthermore, a lack of mafic microgranular enclaves argues against magma mixing. Hence, these felsic rocks were most likely generated by crustal melting.

There are two common settings for melt generation – hydrous and anhydrous –, with the former requiring lower temperatures than the latter (e.g., Weinberg and Hasalová, 2015). High contents in K_2O (Fig. 3A) and HFSEs (Fig. 4A) as well as high calculated values of saturation and crystallization temperatures (Table 3) indicate that felsic rocks of the Piskahegan Group and coeval granites were produced by melting in an anhydrous setting (Weinberg and Hasalová, 2015). This was followed by prolonged fractional crystallization during ascent of the magma, as suggested by high contents in incompatible elements paired with strongly developed Eu anomalies (Figs. 5 and 6) and Sr vs Rb/Sr values (Fig. 7A).

The primitive mantle-normalized plots (Fig. 6) provide further information on the fractional crystallization history of the magma. Distinctly negative Sr, Ba and Eu anomalies reflect the fractional crystallization of feldspars, whereas negative anomalies of Ti and P suggest fractionation of Fe-Ti oxides and apatite. As noted earlier, the Rb/Sr vs Sr plot (Fig. 8A) suggests that the basal succession of the caldera (the Scoullar Mountain, Little Mount Pleasant and Seelys formations) are more fractionated than the subsequent McDougall Brook Granitic Suite and younger volcanic units (the Big Scott Mountain Formation and Bailey Rock Rhyolite). This supports the conclusions of Thorne et al. (2013), who interpreted the Mount Pleasant Caldera Complex as the product of two separate caldera-forming events. Our data suggests that melts associated with the second-generation caldera did not linger in the crust as long prior to their crystallization at depth or eruption as those associated with the first-generation caldera.

The Piskahegan Group rhyolites and associated granites have lower $\varepsilon_{Nd}(t)$ values (-0.10 to +1.05) than those of associated mafic rocks (Fig. 8), which show values ranging from +2.51 to +2.22 (Dostal and Jutras, 2016). Andesites of the Scoullar Mountain Formation have lower $\varepsilon_{Nd}(t)$ values (+ 0.5 to +1.9; Dostal and Jutras, 2016) than the basalts and mostly higher values than the rhyolites (Fig. 8), suggesting that they might be the products of magma mixing. As with all documented igneous rocks in the Avalonian and Ganderian domains, most depleted-mantle model ages (after DePaolo, 1988) obtained from felsic rocks of the Piskahegan Group and coeval granites range between ~800 and ~1,100 Ma (Fig. 8). This suggests that the primary source of crustal rocks in these domains is a sub-continental lithospheric mantle that was metasomatically enriched during the Neoproterozoic (Murphy et al., 2008).

6.3. Geochronology

The newly determined 374.2±2 Ma U-Pb zircon age for the Scoullar Mountain Formation is the oldest so far obtained in the Piskahegan Group. Considering that the Hoyt Station Basalt and Rothea Formation of the Exocaldera Sequence are possibly older based on tentative stratigraphic correlations (McCutcheon et al., 1997), this new date provides an upper limit to the beginning of volcanic activity in the Mount Pleasant caldera complex and its surroundings.

As noted earlier, the Late Caldera-Fill Sequence was previously thought to be younger than both the Intracaldera and Exocaldera sequences (e.g. McCutcheon et al., 1997). However, our new U-Pb zircon date of 365.0±1.8 Ma for the Big Scott Mountain Formation (base of the Late Caldera-Fill Sequence) makes this unlikely, as the Carrow Formation and Bailey Rock Rhyolite of the Exocaldera Sequence yielded U-Pb zircon ages of 363.8 ± 2.2 and 363.4 ± 1.8 Ma, respectively. Given that all three dates overlap within error, the observation that both the Big Scott Mountain Formation and Bailey Rock Rhyolite are concordantly overlain by the Kleef Formation (McCutcheon et al., 1997; Thorne et al., 2013) suggests that they are at least in part coeval. Based on available data, the Big Scott Mountain Formation can therefore be considered as a lateral equivalent of the Carrow Formation and Bailey Rock Rhyolite (Fig. 1).

If granites in the northern part of the caldera are penecontemporaneous with those in the southern part, which are estimated to be no younger than ~370 Ma (Thorne et al., 2013), a significant gap separates them from the ~365 Ma base of the overlying Late Caldera-Fill Sequence, which, as noted earlier, may be associated with a second-generation caldera. Part of this gap may have been filled by nearby plutonic activity in the Mount Douglas Granite within the adjacent Saint-George Batholith, which occupies most of the Kingston Uplift to the south (Fig. 1). This granite yielded crystallization ages of 367±1 Ma based on U–Pb zircon geochronology (Bevier, 1988), and 368±3 Ma based on U–Pb monazite and zircon geochronology (Mohammadi et al., 2020a). Hence, scattered reported ages suggest nearly continuous magmatic activity in the area for most of the Late Devonian.

6.4. Relation between volcanic rocks and granites

Rhyolites of the Piskahegan Group are fractionated leucocratic high-silica rocks, whereas the associated intrusive rocks have a wider range of silica contents (65-78 wt.%; Yang et al., 2003). However, the silica-rich intrusive rocks are compositionally comparable to the rhyolites (Figs. 3-8). The Nd isotopic values and saturation temperatures for both plutonic and volcanic suites also overlap (Tables 2-3). This implies that the rhyolites represent more differentiated parts of the intrusive suites and suggests that only high-silica magma from the top of the successive felsic magma chambers was extruded. Among the plutonic bodies, only the late, small intrusions of the Mount Pleasant Granitic Suite are mineralized and host distinct alteration (greisen) zones (Yang et al., 2003; Thorne et al., 2013). These late intrusions have high silica contents (72 to 77 wt.%), as well as high F, Li and Rb, and low K/Rb (< 60) and Nb/Ta (<8), indicating that fluid fractionation (F-fluxing) was involved during late-stage magmatic differentiation (Yang et al., 2003).

6.5. Mineralization in the Mount Pleasant caldera

The indium-bearing tin-polymetallic deposit that was emplaced in the eruptive centre of Mount Pleasant is associated with granitic intrusions near the southwestern margin of the caldera. The mineralization was generated by magmatic-hydrothermal fluids derived from a silicic magma (Sinclair et al., 2006). The host leucogranites (NB-3 granites of Yang et al. 2003 and Azadbakht et al. 2019) are post-orogenic, peraluminous, low phosphorous and high silica rocks that resemble rare-metal Li-F granites (Gourcerol et al., 2019). The felsic magma evolved through extreme fractional crystallization involving halogens, including F. However, recent experimental data (Michaud et al., 2021) suggest that the distinctive geochemical features of these granitic rocks require not only prolonged fractionation but also mica dehydration melting and probably a distinct source.

6.6. Tectonic Setting

Rhyolites of the Piskahegan Group and associated granites are part of an extensive magmatic province that developed in relation to post-Acadian relaxation paired with the transtensional opening of the Maritimes Basin and subbasins, which gives them affinities with both post-orogenic (Fig. 4C) and within-plate (Fig. 4A-B) felsic rocks. It has been proposed that heat from an overridden plume has contributed to the profuse magmatism that affected southeastern Canada in Late Devonian to Early Carboniferous times (Murphy et al., 1999), although magmatism with a plume signature only started to be recorded in late Visean (late Early Carboniferous) basalts near the centre of the Maritimes Basin (Jutras et al., 2018; Jutras and Dostal, 2019). A similar delay between the timing of plume overriding and the extrusion of plume-derived magma is inferred from the Cenozoic geology of the western United States (Murphy et al., 1998; Murphy, 2016), which is consistent with geodynamic models suggesting that such magma does not easily break through continental lithosphere (McNutt and Fischer, 1987). Heat from the Late Devonian to Early Carboniferous overriding of a plume in eastern Canada may also be responsible for the formation of a ~13 km thick mafic body that currently underlies the entire Maritimes Basin at the base of the crust based on geophysical survey data (Marillier and Verhoef, 1989).

The geochemical signature of most Late Devonian to Tournaisian (earliest Carboniferous) mafic rocks in southeastern Canada suggests a sub-continental lithospheric mantle (SCLM) source that had previously experienced a long history of subduction-related metasomatism (Pe-Piper and Piper, 1998). However, such SCLM signature is less developed in basalts of the Piskahegan Group, which may have been mostly sourced from the asthenosphere (Dostal and Jutras, 2016). Although it is not clear from the geological record if a mantle plume and associated mafic underplating were already present in Late Devonian times, they might be necessary to account for the formation of such profuse felsic magma during that interval. There is, however, no geochemical evidence for significant crystal fractionation or crustal contamination in most of the regional Upper Devonian basalts (e.g. Pe-Piper and Piper, 1998; Dostal and Jutras, 2016), which argues against a long residence time within a sub-crustal mafic underplating prior to their eruption. As inferred by Thybo and Nielsen (2009), mafic underplating can form through a series of relatively small sill injections, which may never become a source for mafic volcanism although associated dykes may reach the surface directly from the base of the lithosphere. The heat derived from such sill injections is most probably responsible for the formation of coeval felsic magma by inducing melting of the lower crust below the Maritimes Basin (Fig. 9).

By late Visean times, the zone of concentrated volcanism had migrated from the southern edge of the Maritimes Basin to the centre of the basin, which has been interpreted as the result of lithospheric migration above the plume (Murphy et al., 1999; Jutras et al. 2018; Jutras and Dostal, 2019) (Fig. 10). In these late stages of the magmatic system, the basin hosted sub-alkaline basalts compositionally similar to enriched mid-oceanic ridge basalts (E-MORBs) sourced from slightly depleted uppermost asthenospheric material (E-DM), which alternate with highly alkaline basalts with a trace element signature that is similar to ocean island basalts (OIBs) sourced from enriched-mantle material, suggesting that two contrasting sources were being tapped-into by different weak zones (Jutras and Dostal, 2019). In peak stages of continental transtension, basalt compositions show evidence of mixing between melts from these two sources, which possibly occurred at the level of a particularly well fed sub-crustal mafic underplating (Jutras and Dostal, 2019) (Fig. 10). The clear geochemical evidence for the involvement of a plume that is provided by highly radiogenic Pb, strongly positive εNd, and OIB-type distribution of trace elements in these Upper Visean volcanic rocks (Pe-Piper and Piper, 1998; La Flèche et al., 1998; Jutras and Dostal, 2019) lends support to the hypothesis that the presence of a plume also contributed to the melting of a very large volume of lower crust material within the same magmatic province in Late Devonian times (Fig. 9).

6.7. Late Devonian biotic crisis in association with the development of a Large Igneous Province in southeastern Canada

Late Devonian to Early Carboniferous igneous rocks are so voluminous in southeastern Canada that an argument can be made that they represent a Large Igneous Province (LIP), especially when considering that a large portion of these rocks is either buried beneath thick Upper Carboniferous to Permian strata, or has been eroded from basement highs. Based on (1) the presence at the centre of the Maritimes Basin of cap rocks cutting through Permian strata above large salt diapirs (Barr et al., 1985), which provide small windows of otherwise deeply buried Lower Carboniferous volcanic strata, and (2) the abundance of Late Devonian to Early Carboniferous granites in basement highs adjacent to the composite basin (e.g. Kellet et al., 2014, 2021), the magmatic province can be considered as encompassing the entire basin and its source areas (i.e.., the entirety of southeastern Canada). This also corresponds to the extent of the ~13 km thick mafic underplating at the base of the crust, which can also be considered part of the LIP.

Large Igneous Provinces can be subdivided into two groups based on the predominance of either mafic or silicic rocks. Mafic LIPs can occur in both continental and oceanic settings and are mainly composed of mafic intraplate rocks that were typically emplaced during a short duration (< 5 My) or characterized by multiple pulses over a maximum of a few 10s of My (e.g., Ernst et al., 2020). Silicic LIPs are exclusively continental and are mainly composed of rhyolites, dacites and felsic volcaniclastic rocks. They are typically eruptive for less than 40 My (e.g., Bryan and Ferrari, 2013). As is the case for the Late Devonian of southeastern Canada, silicic igneous rocks of other LIPs have been interpreted as products of crustal melting from the continuous injection of mafic magma in the crust (e.g. Shellnutt et al., 2013). Such LIPs often coincide with major extinction events (e.g. Ernst et al., 2020; Black and Aiuppa, 2023; Deegan et al., 2023; Grasby and Bond, 2023; Svensen et al., 2023).

Based on a Kernel density plot applied to U-Pb dates obtained from 153 igneous rocks ranging between 420 and 360 Ma in all of southeastern Canada, post-Acadian magmatic activity was most concentrated in the 376-371 Ma interval (Kellet et al., 2021). Our new date of 374.2±2 Ma from near the base of Piskahegan Group paired with the upper limit of ~370 Ma provided by the youngest granites that intrude it, suggests that the entire Intracaldera Sequence contributed to that major pulse of magmatism. Based on McCutcheon et al. (1997), this basal sequence is at least 1650 m thick in the caldera and is incomplete due to the presence of unconformities between the Little Mount Pleasant and Seelys formations, as well as between the latter and the Carrow Formation. This major magmatic pulse between 376 and 371 Ma is of special interest, as it may have contributed to the significant environmental deterioration that led to the Frasnian-Famennian extinction (the Kellwasser event of Walliser, 1986), which is currently dated at 371.1 Ma (Becker et al., 2020).

In terms of volcanic activity, the Maritimes Basin igneous province also contributed a ~1 km thick succession of red beds, basalts and rhyolites assigned to the Fisset Brook Formation in Cape Breton Island, Nova Scotia, from which U-Pb zircon dates of 374±2, 371±3 and 371±2 Ma have been obtained (Dunning et al., 2002). The latter authors also obtained a U-Pb zircon date of 370±1.5 Ma from a rhyolite at the top of the McAras Brook Formation, which is regionally dominated by thick intervals of undated basalts and red beds in northern mainland Nova Scotia. Moreover, although late Frasnian volcanic and sedimentary rocks are only preserved in the West Avalonian and South Ganderian domains, large felsic plutonic bodies have yielded radiometric ages of ~376-371 Ma as remotely as the Humber Zone of eastern Quebec and the Meguma Zone of south and central mainland Nova Scotia (Kellet et al., 2021, and references therein) (Fig. 9). Many of these plutonic bodies must have sourced volcanic rocks that were subsequently eroded.

In some areas of Nova Scotia and its adjacent continental shelf (Meguma Zone), lowermost Carboniferous rocks unconformably overly Late Devonian granites that are estimated to have crystallized at a depth of ~10-12 km (Martel and Gibling, 1996; Kontak and Kyser, 2011; Jamieson et al., 2012), which implies that significant erosion occurred in that area in latest Devonian times. As the Meguma Zone is characterized by the greatest volume of Late Devonian plutons in southeastern Canada, including the South Mountain Batholith (Fig. 1), it can be argued that the bulk of Late Devonian volcanism probably occurred in that area prior to erosion (Fig. 9). In other words, Late Devonian volcanic rocks of the Piskahegan, Harvey and Fountain Lake groups as well as those of the McAras Brook and Fisset Brook formations possibly represent minor peripheral remnants of a large volcanic province that may have been centered in the area of present day southern and central mainland Nova Scotia and its adjacent continental shelf. Significant late Frasnian volcanism may have also occurred as far north as the Humber Zone in association with the McGerrigle Mountains plutonic complex (Fig. 9A) before being subsequently eroded during the long hiatus that separates early Frasnian beds of the Escuminac Formation from Visean red beds in that area.

Although these volcanic activities may not be exclusively responsible for the Frasnian-Famennian extinction, they must have significantly contributed to global shifts in environmental conditions, particularly when the climate was near a tipping point (e.g., Ernst et al., 2020). Furthermore, recent research has underlined the especially detrimental effects of LIP magmas intruding sedimentary rocks (e.g. Black and Aiuppa, 2023; Deegan et al., 2023; Grasby and

Bond, 2023; Svensen et al., 2023), which constitute the bulk of pre-Acadian basement rocks and their successor basins in southeastern Canada (e.g., Gibling et al., 2019).

7. Conclusions

Felsic volcanic rocks of the Piskahegan Group and intraformational granites form a major part of a late Paleozoic caldera complex that hosts a significant polymetallic deposit of tin, tungsten, molybdenum, indium, and bismuth. Mineralization is associated with strongly fractionated and altered granitic plutons of the Mount Pleasant Granitic Suite, which intruded the lower part of the caldera-fill as well as larger, penecontemporaneous plutons of the McDougall Brook Granitic Suite (Thorne et al., 2013).

The Mount Pleasant caldera complex formed during the initial opening of the southwestern part of the composite, late Paleozoic Maritimes Basin. The caldera is largely composed of bimodal volcanic rocks derived from two distinct sources: mantle-derived mafic magmas and crust-derived felsic magmas. The oldest dated felsic volcanic rocks (the Scoullar Mountain Formation) provide an upper limit to the beginning of volcanic activity in the Mount Pleasant caldera complex at 374.2 ±2 Ma, whereas the uppermost dated volcanic unit of the complex (the Big Scott Mountain Formation) yielded an age of 364.6±0.7 Ma. In the caldera, granitic plutons intruded the lower part of the succession (Intracaldera Sequence of McCutcheon et al., 1997), culminating around 370 Ma (Thorne et al., 2013). These granitic bodies and the Intracaldera Sequence are unconformably overlain by the upper part of the caldera succession (Late Caldera-Fill Sequence of McCutcheon et al., 1997), which starts with the Big Scott Mountain Formation.

Felsic rocks from the entire caldera succession and adjacent Exocaldera Sequence are fractionated, post-orogenic, peraluminous A-2 type rocks with volatile-free silica contents ranging from 70.2 to 78.7 wt.%, and with high K_2O as well as low CaO, FeO_t, MgO, TiO_2 and P_2O_5 (Table 1). These rocks are interpreted to have been generated by the high-temperature melting of lower crust material. The rhyolites are compositionally similar to the more differentiated parts of the mid-sequence intrusions, suggesting that they were extruded from a similar magma chamber. Their $\varepsilon_{Nd}(t)$ values range between +0.33 and +0.95 (Table 2; -0.10 to +1.05 based on Anderson, 1992, and Whalen et al., 1996), which places them within the Avalonian/Ganderian envelope (per Murphy et al., 2008, and Dostal et al., 2021, 2022). The felsic melts are interpreted to have been triggered by the continuous injection of mantle-derived mafic sills at the base of the crust (Fig. 9). Over time, these magma injections produced a ~13 km thick sub-crustal mafic body that is as laterally extensive as the entire Maritimes Basin and its source areas (Marillier and Verhoef, 1989).

Late Devonian to Early Carboniferous igneous rocks in southeastern Canada are so voluminous that they can be regarded as part of a LIP. Their large volume has led to the hypothesis that they are associated with the presence of an underlying mantle plume that was being overridden by the Canadian Appalachian lithosphere (Murphy et al., 1999). This is supported by the eventual appearance of mafic rocks with an OIB signature in late stages of the magmatic system (Fig. 10; Jutras et al., 2018; Jutras and Dostal, 2019). However, early stages were marked by more profuse magmatism, especially when considering that an estimated ~10-12 km of erosion occurred in latest Devonian times (based on inferences from Martel and Gibling, 1996, Kontak and Kyser, 2011, and Jamieson et al., 2012), which must have eradicated most of the original volume of extrusive rocks. Whereas most of the Late Devonian magmatism occurred too early to have been of influence at the time of the terminal Devonian extinction, there is a large volume of late Frasnian volcanic rock remnants in the Piskahegan Group of New Brunswick as well as in the McAras Brook and Fisset Brook formations of Nova Scotia, which is associated with a much greater volume of coeval intrusive rocks (Kellett et al., 2021, and references therein) that most likely contributed the bulk of volcanic rocks in that time period prior to their erosion in late Famennian times. It is also likely that this episode of profuse late Frasnian magmatism in southeastern Canada contributed significantly to the environmental deterioration that led to the Kellwasser Event at the Frasnian-Famennian boundary.

Acknowledgements

This research was supported by NSERC (Canada) Discovery grants to J. Dostal and P. Jutras and CONACYT Grant #7351 to L. Solari. We thank Carlos Ortega-Obregón for maintaining the LA-ICPMS facilities at CGEO, UNAM. We also thank Dr. John Greenough and an anonymous reviewer for careful reviews that helped expand the scope of the manuscript and improve its clarity, as well as Dr. Ali Polat for his editorial handling.

References

Ackerman, L., Žák, K., Skála, R., Rejšek, J., Křížová, Š., Wimpenny, J., Magna, T., 2020. Sr–Nd–Pb isotope systematics of Australasian tektites: Implications for the nature and composition of target materials and possible volatile loss of Pb. Geochimica et Cosmochimica Acta 276, 135–150.

Anderson, H.E., 1992. A chemical and isotopic study of the age, petrogenesis and magmatic evolution of the Mount Pleasant caldera complex, New Brunswick. PhD thesis, Carleton University, Ottawa, Ontario

Azadbakht, Z., Rogers, N., Lentz, D.R., McFarlane, C.R.M., 2019. Petrogenesis and associated mineralization of Acadian related granitoids in New Brunswick. In: Rogers, N. (Ed.). Targeted Geoscience Initiative: 2018 report of activities. Geological Survey of Canada, Open File 8549, 243–278.

Barr, S. M., Brisebois, D., Macdonald, A. S., 1985. Carboniferous volcanic rocks of the Magdalen Islands, Gulf of St. Lawrence. Canadian Journal of Earth Sciences 22,1679–1688.

Becker, R. T., Marshall, J. E. A., Da Silva, A. C., Agterberg, F. P., Gradstein, F. M., Ogg, J. G., Schmitz, M. D., 2020. Geologic Time Scale, The Devonian Period. Elsevier: Amsterdam, The Netherlands, pp. 733–810.

Bevier, M.L., 1988. U–Pb geochronologic studies of igneous rocks in New Brunswick. In: Abbott, S.A. (Ed.). Thirteenth Annual Review of Activities. New Brunswick Department of Natural Resources and Energy, Minerals and Energy Division, Information Circular Vols. 88-2, 134–140.

Black, B.A., Aiuppa, A., 2023. Carbon release from Large Igneous Province magmas estimated from trace element-gas correlations. Volcanica 6, 129-145.

Boehnke, P., Watson, E.B., Trail, D., Harrison, T.M., Schmitt, A.K., 2013. Zircon saturation re-revisited. Chemical Geology 351, 324–334.

Bonin, B., 2007. A-type granites and related rocks: evolution of a concept, problems and prospects. Lithos 97, 1–29.

Boynton, W.V., 1984. Cosmochemistry of the rare earth elements; meteorite studies. In: Henderson, P. (Ed.) Rare Earth Element Geochemistry, Elsevier: Amsterdam, The Netherlands, 63–114.

Bowen, N.L., 1928. Evolution of Igneous Rocks. Princeton University Press, Princeton.

Bryan, S.E., Ferrari, L., 2013. Large igneous provinces and silicic large igneous provinces: progress in our understanding over the last 25 years. Geological Society of America Bulletin 125, 1053-1078.

Corfu, F., Hanchar, J.M., Hoskin, P.W.O., Kinny, P., 2003. Atlas of Zircon Textures. Reviews of Mineralogy and Geochemistry 53, 469–500.

Deegan, F.M., Callegaro, S., Davies, J.H., Svensen, H.H., 2023. Driving global change one LIP at a time. Elements 19, 269-275.

DePaolo, D.J., 1988, Neodymium Isotope Geochemistry: An Introduction. New York, Springer Verlag. 187 p.

Dostal, J., Jutras, P., 2016. Upper Paleozoic mafic and intermeditate volcanic rocks of the Mount Pleasant caldera associated with the Sn-W deposit in southwestern New Brunswick (Canada): Petrogenesis and metallogenic implications. Lithos 262, 428-441.

Dostal, J., Keppie, J.D., Jutras, P., Miller, B.V., Murphy, J.B., 2006. Evidence of the granulite-granite connection: Penecontemporaneous high-grade metamorphism, granitic magmatism and core complex development in the Liscomb Complex, Nova Scotia, Canada. Lithos 86, 77-90.

Dostal, J., van Hengstum, T.R., Shellnutt, J.G., Hanley, J.J., 2016. Petrogenetic evolution of Late Paleozoic rhyolites of the Harvey Group, southwestern New Brunswick (Canada) hosting uranium mineralization. Contributions to Mineralogy and Petrology 171, 59.

Dostal, J., Wilson, R.A., Jutras, P., 2021. Petrogenesis of Siluro-Devonian rhyolites of the Tobique Group in the northwestern Appalachians (northern New Brunswick, Canada): tectonic implications for the accretion history of peri-Gondwanan terranes along the Laurentian margin. Geological Society, London, Special Publications 503, 391-407.

Dostal, J., Jutras, P., Wilson, R.A., 2022. Geochemical and Nd isotopic constraints on the origin of the uppermost Silurian rhyolitic rocks in the northern Appalachians (northern New

Brunswick): Tectonic implications. In: Kupier, Y. D., Murphy, J. B., Nance, R.D., Strachan, R.A., Thompson, M.D. (Eds). New Developments in the Appalachian-Caledonian-Variscan Orogen. Geological Society of America Special Paper 554, 121-122.

Dunning, G.R., Barr, S.M., Giles, P.S., McGregor, D.C., Pe-Piper, G., Piper, D.J.W., 2002. Chronology of Devonian to early Carboniferous rifting and igneous activity in southern Magdalen Basin based on U-Pb (zircon) dating. Canadian Journal of Earth Sciences 39, 1219-1237.

Eby, N., 1992. Chemical subdivision of the A-type granitoids: Petrogenetic and tectonic implications. Geology 20, 641–644.

Ernst, R.E., Rodygin, S.A., Grinev, O.M., 2020. Age correlation of Large Igneous Provinces with Devonian biotic crises. Global and Planetary Change 185, 103097.

Ferry, J. M., Watson, E. B., 2007. New thermodynamic models and revised calibrations for the Ti-in-zircon and Zr-in-rutile thermometers. Contributions to Mineralogy and Petrology 154, 429–437.

Frost, B.R., Frost, C.D., 2008. A geochemical classification for feldspathic igneous rocks. Journal of Petrology 49, 1955-1969.

Frost, B.R., Barnes, C.G., Collision, W.J., Arculus, R.J., Ellis, D.J., Frost, C.D., 2001. A geochemical classification for granitic rocks. Journal of Petrology 42, 2033-2048.

Gibling, M.R., Culshaw, N., Pascucci, V., Waldron, J.W.F., Rygel, M.C., 2019. The Maritimes Basin of Atlantic Canada: Basin creation and destruction during the Paleozoic assembly of Pangea. In: The sedimentary basins of the United States and Canada. Elsevier: Amsterdam, The Netherlands, pp. 267-314.

Grasby, S.E., Bond, D.P., 2023. How large igneous provinces have killed most life on Earth—numerous times. Elements 19, 276-281.

Gray, T.R., Hanley, J.J., Dostal, J., Guillong, M., 2011. Magmatic enrichment of uranium, thorium and rare earth elements in late Paleozoic rhyolites of southern New Brunswick, Canada: evidence from silicate melt inclusions. Economic Geology 106,127–143.

Harrison, T.M., Watson, E.B., 1984. The behavior of apatite during crustal anatexis. Equilibrium and kinetic considerations. Geochimica et Cosmochimica Acta 48, 1467-1478.

Jahn, B.M., Wu, F.Y., Capdevila, R., Martineau, F., Wang, Y.X., Zhao, Z.H., 2001. Highly evolved juvenile granites with tetrad REE patterns: the Woduhe and Baerzhe granites from the Great Xing'an (Khingan) Mountains in NE China. Lithos 59, 171–198.

Jamieson, R.A., Hart, G.G., Chapman, G.G., Tobey, N.W., 2012. The contact aureole of the South Mountain Batholith in Halifax, Nova Scotia: geology, mineral assemblages, and isograds. Canadian Journal of Earth Sciences 49, 1280–1296.

Jutras, P., Dostal, J., 2019. The Upper Visean Magdalen Islands Basalts of Eastern Quebec, Canada: a Complex Assemblage of Contrasting Mafic Rock Types Erupted in Peak Stages of Transtensional Basin Development above a Mantle Plume. Journal of Geology 127, 505–526.

Jutras, P., Dostal, J., 2023. Late Ordovician to Early Devonian tectono-magmatic prequel to the Acadian Orogeny in northeastern North America and the British Isles. Gondwana Research 124, 378–400.

Jutras, P., Dostal, J., Kamo, S., Matheson, Z., 2018. Tectonostratigraphic and petrogenetic setting of late Mississippian volcanism in eastern Canada. Canadian Journal of Earth Sciences 55, 356-372.

Keller, C.B., Schoene, B., Barboni, M., Samperton, K.M., Husson, J.M., 2015. Volcanic–plutonic parity and the differentiation of the continental crust. Nature 523, 301-307.

Kellett, D.A., Rogers, N., McNicoll, V., Kerr, A., van Staal, C., 2014. New age data refine extent and duration of Paleozoic and Neoproterozoic plutonism at Ganderia-Avalonia boundary, Newfoundland. Canadian Journal of Earth Sciences 51, 943-972.

Kellett, D. A., Piette-Lauziere, N., Mohammadi, N., Bickerton, L., Kontak, D., Rogers, L., 2021. Spatio-temporal distribution of Devonian post-accretionary granitoids in the Canadian Appalachians: implications for tectonic controls on intrusion-related mineralization. Bulletin 2021, Geological Survey of Canada, 7-23.

Keppie, J.D., 2000. Geological map of the Province of Nova Scotia, Map ME 2000-1. Nova Scotia Department of Natural Resources, Halifax, NS, Canada.

Keppie, J. D., Dostal, J., Murphy, J.B., Cousens, B.L., 1997. Palaeozoic within-plate volcanic rocks in Nova Scotia (Canada) reinterpretation: isotopic constraints on magmatic source and palaeocontinental reconstructions. Geological Magazine 134, 425–447.

King, P.L., White, A.J.R., Chappel, B.W., Allen, C.M., 1997. Characterization and origin of aluminous A-type granites from the Lachlan Fold Belt, southeastern Australia. Journal of Petrology 38, 371-391.

Kontak, D.J., Kyser, T.K., 2011. Fingerprinting multiple fluid reservoirs in a 380 Ma Intrusion-Related Gold (IRG) setting, Nova Scotia, Canada: implications for the nature and origin of IRG deposits. Mineralium Deposita 46, 337–363.

La Flèche, M.R., Camiré G., Jenner, G.A., 1998. Geochemistry of post-Acadian, Carboniferous continental intraplate basalts from the Maritimes Basin, Magdalen Islands, Québec, Canada. Chemical Geology 148, 115–136.

Lundstrom, C.C., Glazner, A.F., 2016. Silicic magmatism and the volcanic–plutonic connection. Elements 12, 91–96.

Maniar, P.D., Piccoli, P.M., 1989. Tectonic discrimination of granitoids. Geological Society of America Bulletin 101, 635-643.

Marillier, F., Verhoef, J., 1989. Crustal thickness under the Gulf of St. Lawrence, northern Appalachians, from gravity and deep seismic data. Canadian Journal of Earth Sciences 26, 1517-1532.

Martel, A.T., Gibling, M.R., 1996. Stratigraphy and tectonic history of the upper Devonian to lower Carboniferous Horton Bluff Formation, Nova Scotia. Atlantic Geology 32, 13-38.

Marsh, B.D., 2006. Dynamics of magmatic systems. Elements 2, 287-292.

McBirney, A.R. 2006. Igneous Petrology. 3rd ed. Jones &Bartlett, Sudbury, M, 550 p.

McCutcheon, S.R., Anderson, H.E., Robinson, P.T., 1997. Stratigraphy and eruptive history of the Late Devonian Mount Pleasant Caldera Complex, Canadian Appalachians. Geological Magazine 134, 17–36. McDonough, W.F., Sun, S.-S., 1995. The composition of the Earth. Chemical Geology 120, 229–253.

McGregor, D.C., McCutcheon, S.R., 1988. Implications of spore evidence for Late Devonian age of the Piskahegan Group, southwestern New Brunswick. Canadian Journal of Earth Sciences 25, 1349–1364.

McLeod, M.J., Smith, E.A., 2010. Uranium. New Brunswick Department of Natural Resources; Lands, Minerals and Petroleum Division, Mineral Commodity Profile No. 6, 7 pp.

McNutt, M. K., Fischer, K. M., 1987, The South Pacific superswell, seamounts, islands and atolls: American Geophysical Union Geophysical Monograph 43, 25–34.

Miller, C.F., McDowell, S.M., Mapes, R.W., 2003. Hot and cold granites? Implications of zircon saturation temperatures and preservation of inheritance. Geology 31, 529–532.

Mohammadi, N., McFarlane, C.R.M., Lentz, D.R., Thorne, K.G., 2020a. Timing of magmatic crystallization and Sn-W-Mo greisen vein formation within the Mount Douglas Granite, New Brunswick. Canadian Journal of Earth Sciences 57, 814-839.

Mohammadi, N., Lentz, D.R., McFarlane, C.R.M., Cousens, B., 2020b. Geochemistry of the highly evolved Sn-W-Mo-bearing Mount Douglas Granite, New Brunswick, Canada: implications for origin and mineralization. Ore Geology Reviews 117,103266.

Montel, J.M., 1993. A model for monazite/melt equilibrium and application to the generation of granitic magmas. Chemical Geology 110, 127– 146.

Murphy, J.B., 2016. The role of the ancestral Yellowstone plume in the tectonic evolution of the western United States. Geoscience Canada 43, 231-250.

Murphy, J. B., Oppliger, G. L., Brimhall, G. H., Jr., Hynes, A., 1998, Plume-modified orogeny: An example from the western United States. Geology 26, 731–734.

Murphy, J.B., van Staal, C.R., Keppie, J.D., 1999. Middle to late Paleozoic Acadian orogeny in the northern Appalachians: A Laramide-style plume-modified orogeny? Geology 27, 653-656.

Murphy, J. B., Dostal, J., Keppie, J.D., 2008. Neoproterozoic–Early Devonian magmatism in the Antigonish Highlands, Avalon terrane, Nova Scotia: tracking the evolution of the mantle and crustal sources during the evolution of the Rheic Ocean. Tectonophysics 461, 181-201.

Namur, O., Charler, B., Toplis, M.J., Higgins, M.D., Hounsell, V., Liegeois, J.P., Auwera, J.V., 2011. Differentiation of tholeiitic basalt to A-type granite in the Sept Iles layered intrusion, Canada. Journal of Petrology 52, 487-539.

Narshimha, C., Kumar, S., 2023. Peraluminous A-type granites formed through synchronous fractionation, magma mixing, mingling, and undercooling evidence from microgranular enclaves and host Mesoproterozoic Kanigiri granite pluton, Nellore Schist Belt, southeast India. Acta Geochimica 42, 603–636.

New Brunswick Department of Natural Resources and Energy, 2000. Bedrock geology of New Brunswick. Minerals and Energy Division, Map NR-1 (2000 Edition). Scale 1:500 000.

Papoutsa, A., Pe-Piper, G., Piper, D.J.W., 2016. Systematic mineralogical diversity in A-type granitic intrusions: Control on magmatic source and geological processes. Geological Society of America Bulletin 128, 487-501.

Paton, C., Woodhead, J.D., Hellstrom, J.C., Hergt, J.M., Greig, A., Maas, R., 2010. Improved laser ablation U-Pb zircon geochronology through robust downhole fractionation correction. Geochemistry, Geophysics, Geosystems 11, 3.

Pearce, J., 1996. Sources and settings of granitic rocks. Episodes 19, 120-125.

Pe-Piper, G., Piper, D.J.W., 1998. Geochemical evolution of Devonian–Carboniferous igneous rocks of the Magdalen Basin, Eastern Canada: Pb-and Nd-isotope evidence for mantle and lower crustal sources. Canadian Journal of Earth Sciences 35, 201–221.

Peccerillo, A., Taylor, S.R., 1976. Geochemistry of Eocene Calc-Alkaline Volcanic Rocks from the Kastamonu Area, Northern Turkey. Contributions to Mineralogy and Petrology 58, 63-81.

Petrus, J. A., Kamber, B. S., 2012. VizualAge: A Novel Approach to Laser Ablation ICP-MS U-Pb Geochronology Data Reduction. Geostandards and Geoanalytical Research 36, 247-270.

Pollock, J.C., Sylvester, P.J., Barr, S.M., 2015. Lu–Hf zircon and Sm–Nd whole-rock isotope constraints on the extent of juvenile arc crust in Avalonia: examples from Newfoundland and Nova Scotia, Canada. Canadian Journal of Earth Sciences 52, 161–181.

Ruffman, A., Greenough, J.D., 1990. The Weekend dykes, a newly recognized mafic dyke swarm on the eastern shore of Nova Scotia, Canada. Canadian Journal of Earth Sciences 27, 644-648.

Schiller, D., Finger, F., 2019. Application of Ti-in-zircon thermometry to granite studies: Problems and possible solutions. Contributions to Mineralogy and Petrology 174, 51.

Shellnutt, J.G., Bhat, G.M., Wang, K.L., Brookfield, M.E., Dostal, J., Jahn, B.M., 2012. Origin of the silicic volcanic rocks of the Early Permian Panjal Traps, Kashmir, India. Chemical Geology 334, 154-170.

Sinclair, W.D., Kooiman, G.J.A., Martin, D.A., Kjarsgaard, I.M., 2006. Geology, geochemistry and mineralogy of indium resources at Mount Pleasant, New Brunswick, Canada. Ore Geology Reviews 28, 123-145.

Sláma, J., and 13 others, 2008. Plešovice zircon- new natural reference material for U-Pb and Hf isotopic microanalysis. Chemical Geology 249, 1-35.

Sliwinski, J. T., Guillong, M., Horstwood, M. S. A., Bachmann, O., 2022. Quantifying Long-Term Reproducibility of Zircon Reference Materials by U-Pb LA-ICP-MS Dating. Geostandards and Geoanalytical Research 46, 401–409.

Solari, L. A., González-León, C.M., Ortega-Obregón, C., Valencia-Moreno, M., Rascón-Heimpel, M.A., 2018. The Proterozoic of NW Mexico revisited: U–Pb geochronology and Hf isotopes of Sonoran rocks and their tectonic implications. International Journal of Earth Sciences 107, 845-861.

Solari, L. A., Torres de León, R., Hernández Pineda, G., Sole, J., Solis-Pichardo, G., Hernández-Trevino, T., 2007. Tectonic significance of Cretaceous -Tertiary magmatic and structural evolution of the northern margin of the Xolapa Complex, Tierra Colorada area, southern Mexico. Geological Society of America Bulletin 119, 1265-1279.

Svensen, H.H., Jones, M.T., Mather, T.A., 2023. Large igneous provinces and the release of thermogenic volatiles from sedimentary basins. Elements 19, 282-288.

Thorne, K.G., Fyffe, L.R., Creaser, R.A., 2013. Re–Os geochronological constraints on the mineralizing events within the Mount Pleasant Caldera: implications for the timing of subvolcanic magmatism. Atlantic Geology 49, 131–150.

Thybo, H., Nielsen, C.A., 2009. Magma-compensated crustal thinning in continental rift zones. Nature 457, 873-876.

Tucker, R.D., Bradley, D.C., Ver Straeten, C.A., Harris, A.G., Ebert, J.R., McCutcheon, S.R., 1998. New U–Pb zircon ages and the duration and division of Devonian time. Earth and Planetary Science Letters 158, 175–186.

Yang, X.-M., Lentz, D.R., McCutcheon, S.R., 2003. Petrochemical evolution of subvolcanic granitoid intrusions within the Late Devonian Mount Pleasant Caldera, southwestern New Brunswick, Canada: comparison of Au versus Sn-W-Mo-polymetallic mineralization systems. Atlantic Geology 39, 97–121.

van Staal, C.R., Whalen, J.B., Valverde-Vaquero, P., Zagorevski, A., Rogers, N., 2009. Pre-Carboniferous, episodic accretion-related, orogenesis along the Laurentian margin of the northern Appalachians. Geological Society, London, Special Publications 327, 271–316.

van Staal, C. R., Barr, S.M., Murphy, J.B., 2012. Provenance and tectonic evolution of Ganderia: Constraints on the evolution of the Iapetus and Rheic oceans. Geology 40, 987–990.

Walliser, O.H., 1986. Global Bio-Events: A Critical Approach. Proceedings of the First International Meeting of the IGCP Project 216, p. 1-4. Springer Berlin Heidelberg.

Watson, E.B., Harrison, T.M., 1983. Zircon saturation revisited: Temperature and composition effects in a variety of crustal magma types. Earth and Planetary Science Letters 64, 295–304.

Weinberg, R.F., Hasalová, P., 2015. Water-fluxed melting of the continental crust: A review. Lithos 212–215, 158–188.

Whalen, J.B., Currie, K.L., Chappell, B.W., 1987. A-type granites: Geochemical characteristics, discrimination and petrogenesis. Contributions to Mineralogy and Petrology 95, 407–419.

Whalen, J.B., Fyffe, L.R., Longstaffe, F.J., Jenner, G.A., 1996. The position and nature of the Gander–Avalon boundary, southern New Brunswick, based on geochemical and isotopic data from granitoid rocks. Canadian Journal of Earth Sciences 33, 129-139.

Table captions

Table 1

Major and trace element data.

Table 2

Nd isotopic composition of Piskahegan Group rhyolites and associated granite.

Table 3

Saturation temperatures.

Figure captions

Fig. 1. A – Simplified geological map of Atlantic Canada showing the Appalachian domains and the boundaries of the Late Devonian to Early Permian Maritimes Basin, as well as the location of Upper Devonian intrusive and extrusive units (based on Keppie, 2000, New Brunswick Department of Natural Resources and Energy, 2000, van Staal et al., 2009, Kellett et al., 2021, and Jutras et al., 2023) in Quebec (QC): McGerrigle Mountains; in New Brunswick (NB): the Piskahegan (P) and Harvey (H) groups, and the Mount Douglas Granite (MD), and in Nova Scotia (NS): the Fountain Lake Group (FL) and the Fisset Brook Formation (FB), as well as the South Mountain Batholith (SMB). PEI: Prince-Edward Island. KU: Kingston Uplift. HR: Hardwood Ridge basalts (Carboniferous). B -- Geology of the Mount Pleasant caldera and adjacent extracaldera succession (modified from Thorne et al., 2013); keyed to figure C. C -- Late Devonian stratigraphy of the study area (Epoch boundaries after the Subcommission on Devonian Stratigraphy of the International Commission on Stratigraphy, 2024),

Fig. 2. U-Pb zircon Concordia diagram of two dated samples (A-NB07-32 – Big Scott Mountain Formation rhyolite; B - NB07-66 - Scoullar Mountain Formation rhyolite). All error ellipses and reported ages are at 2-sigma. The inset in each concordia shows the average $^{206}Pb/^{238}U$ ages obtained by pooling the chosen zircon grains.

Fig. 3. Major element characteristics of felsic volcanic rocks of the Piskahegan Group and associated granites. A -- K_2O versus SiO_2 (wt.%) diagram of Peccerillo and Taylor (1976) discriminating between calc-alkaline, high-K, and shoshonitic rocks. B -- Na_2O+K_2O vs SiO_2 (wt.%) diagram of Frost et al. (2001) discriminating between alkalic, alkali-calcic and calc-alkalic compositions. C -- Plot of molar $Al_2O_3/(Na_2O+K_2O)$ [A/NK] vs $Al_2O_3/(CaO+Na_2O+K_2O)$ [A/CNK] (after Maniar and Piccoli, 1989) that discriminates between metaluminous, peraluminous and peralkaline compositions. D -- $FeO_t/(FeO_t+MgO)$ vs SiO_2 (wt.%) diagram of Frost and Frost (2008) discriminating between ferroan (A-type) and magnesian rocks.

Fig. 4. Major and trace element characteristics of felsic volcanic rocks of the Piskahegan Group and associated granites. A -- $(K_2O+Na_2O)/CaO$ (wt. %) vs Zr+Nb+Ce+Y (ppm) diagram of Whalen et al., (1987) discriminating between A-type and M-, I- & S-type felsic rocks. B -- Nb vs Y vs Ce ternary diagram of Eby (1992) discriminating between A1- and A2-type felsic rocks. C -- Nb+Y vs Rb (ppm) tectonic discrimination diagram of Pearce (1996) discriminating between syn-orogenic granites (SOG), volcanic arc granite (VAG), within-plate granite (WPG), ocean ridge granite (ORG) and post-orogenic granite (POG).

Fig. 5. Chondrite-normalized REE average plots for five felsic rock formations of the Piskahegan Group as well as the McDougall Brook Granitic Suite. Normalizing values are after Boynton (1984).

Fig. 6. Primitive mantle-normalized trace element average plots for five felsic rock formations of the Piskahegan Group as well as the McDougall Brook Granitic Suite. Normalizing values are after McDonough and Sun (1995). Elements are arranged in the order of decreasing incompatibility from left to right.

Fig. 7. A -- Rb/Sr vs Sr (ppm) diagram for the felsic volcanic rocks of the Piskahegan Group and associated granites. The vector depicts the trend of compositional changes in the residual liquid as feldspars are progressively removed from the magma during fractional crystallization. B – Th/Yb vs SiO_2 (wt.%) diagram for the rocks of Scoullar Mountain Formation.

Fig. 8. $\varepsilon_{Nd}(t)$ vs time plot comparing Sm-Nd isotopic data of the Piskahegan Group and associated granites with other volcanic rocks in the Avalonian and Ganderian domains of southeastern Canada (Murphy et al., 2008; Dostal et al., 2016, 2021, 2022). The Grenvillian envelope is from Murphy et al. (2008) and references therein. CHUR – chondritic uniform reservoir.

Fig. 9. Tectonic and petrogenetic model for Late Devonian magmatism in southeastern Canada. The model (based on Marillier and Verhoef, 1989, Whalen et al., 1996, Pe-Piper and Piper, 1998, Murphy et al., 1999, Dostal and Jutras, 2016, Jutras and Dostal, 2019, and this study) involves the presence of a mantle plume overridden by the composite Canadian Appalachian lithosphere. The plume would have provided sufficient heat for profuse mafic magma from possibly three distinct mantle sources to be injected at the base of the crust and generate lower crustal melting.

Fig. 10. Tectonic and petrogenetic model for peak late Visean (late Early Carboniferous) magmatism in southeastern Canada (modified from Jutras and Dostal, 2019).

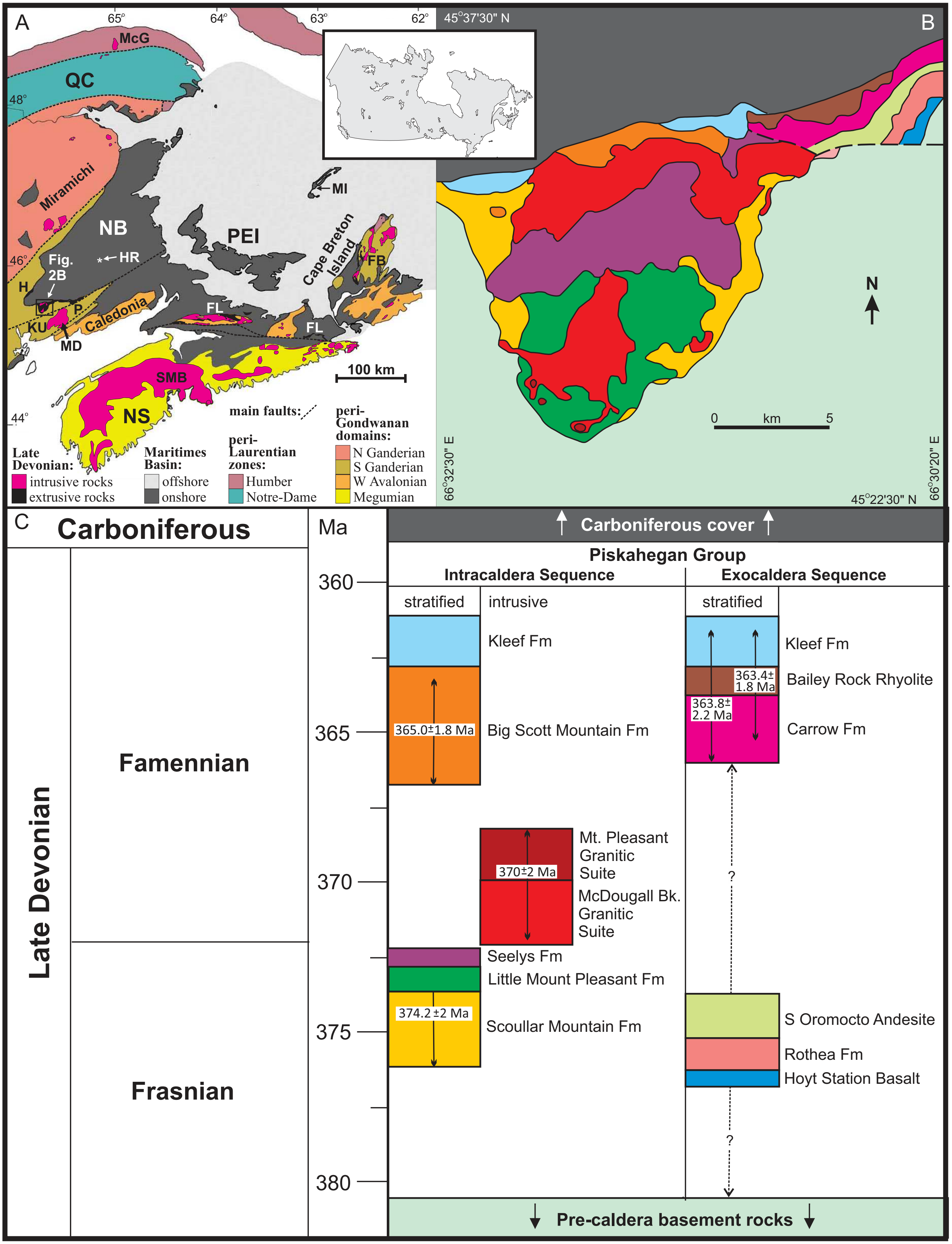
A
65°
64°
63°
62°
McG
QC
48°
Miramichi
NB
PEI
MI
Cape Breton Island
FB
46°
Fig. 2B
HR
H
P
KU
MD
Caledonia
FL
FL
SMB
NS
100 km
44°
main faults:
Late Devonian:
intrusive rocks
extrusive rocks
Maritimes Basin:
offshore
onshore
peri-Laurentian zones:
Humber
Notre-Dame
peri-Gondwanan domains:
N Ganderian
S Ganderian
W Avalonian
Megumian
B
45°37'30" N
N
0 km 5
66°32'30" E
66°30'20" E
45°22'30" N
C
Carboniferous
Late Devonian
Famennian
Frasnian
Ma
360
365
370
375
380
Carboniferous cover
Piskahegan Group
Intracaldera Sequence
Exocaldera Sequence
stratified
intrusive
stratified
Kleef Fm
Big Scott Mountain Fm
365.0±1.8 Ma
Mt. Pleasant Granitic Suite
370±2 Ma
McDougall Bk. Granitic Suite
Seelys Fm
Little Mount Pleasant Fm
Scoullar Mountain Fm
374.2 ±2 Ma
Kleef Fm
Bailey Rock Rhyolite
363.4± 1.8 Ma
Carrow Fm
363.8± 2.2 Ma
?
S Oromocto Andesite
Rothea Fm
Hoyt Station Basalt
?
Pre-caldera basement rocks

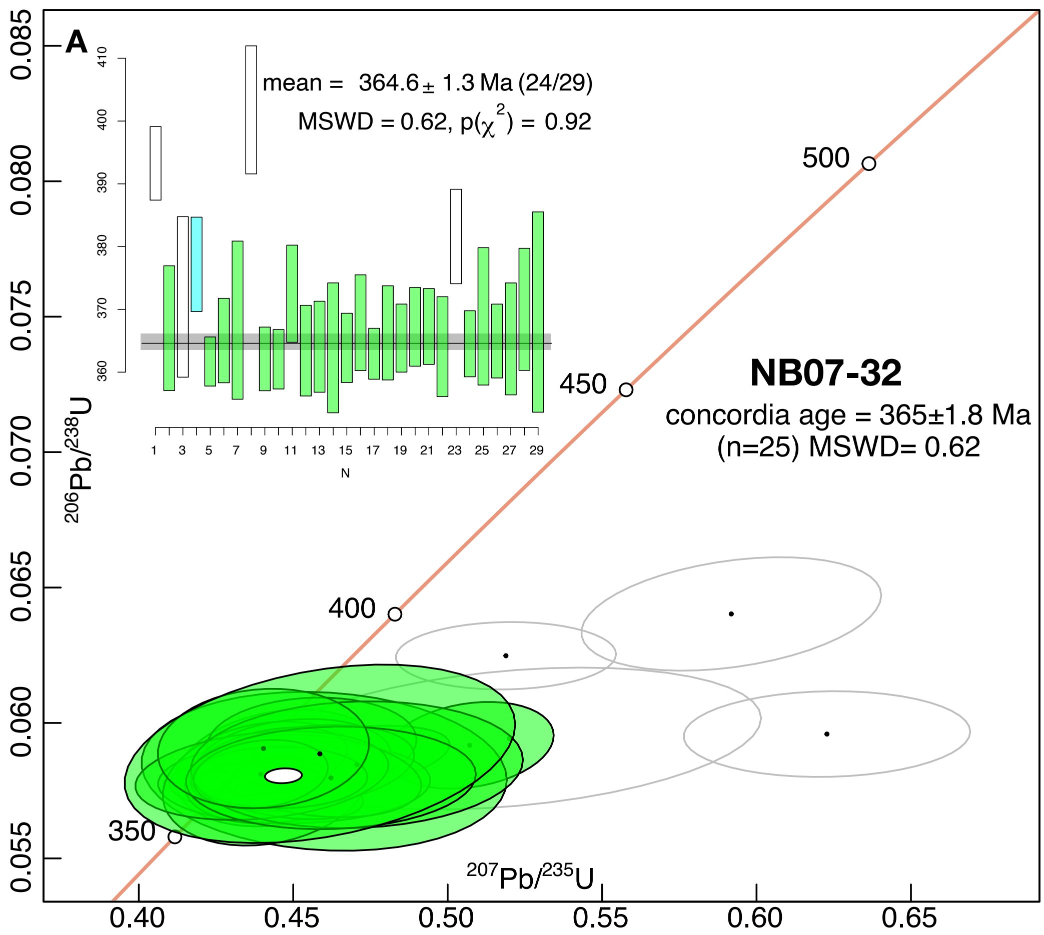
A
mean = 364.6 ± 1.3 Ma (24/29)
MSWD = 0.62, p(χ^2) = 0.92
NB07-32
concordia age = 365±1.8 Ma
(n=25) MSWD= 0.62
$^{206}Pb/^{238}U$
$^{207}Pb/^{235}U$
N

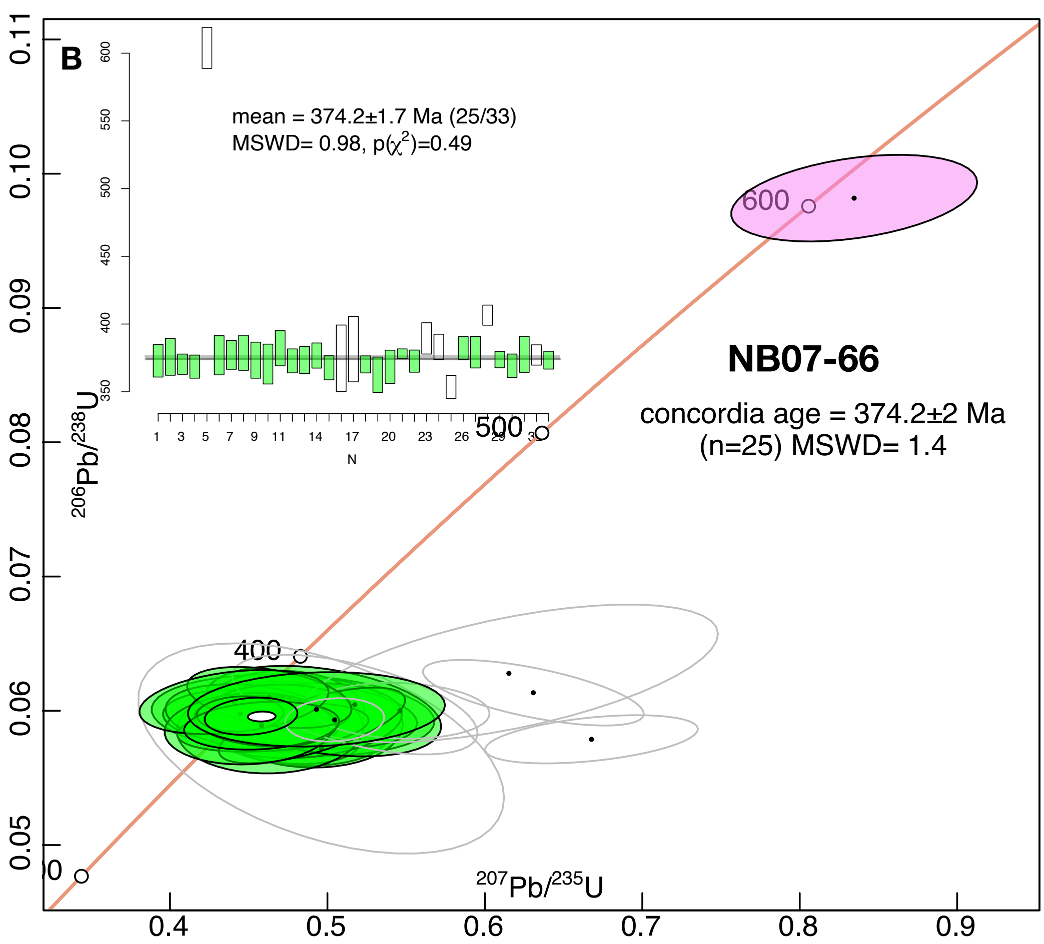
B
mean = 374.2±1.7 Ma (25/33)
MSWD= 0.98, p(χ^2)=0.49
NB07-66
concordia age = 374.2±2 Ma
(n=25) MSWD= 1.4
$^{206}Pb/^{238}U$
$^{207}Pb/^{235}U$
N

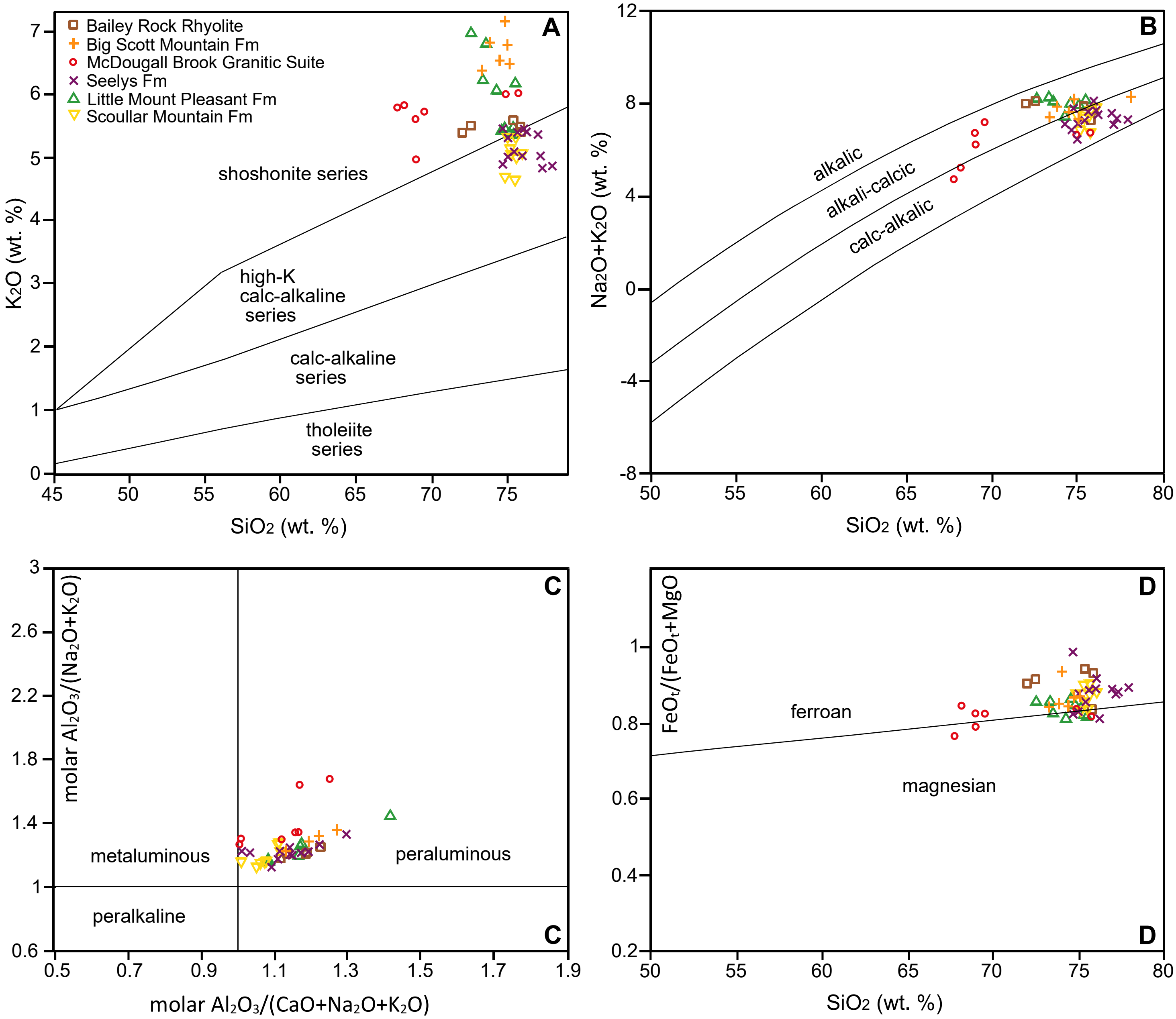
Bailey Rock Rhyolite
Big Scott Mountain Fm
McDougall Brook Granitic Suite
Seelys Fm
Little Mount Pleasant Fm
Scoullar Mountain Fm
A
shoshonite series
high-K calc-alkaline series
calc-alkaline series
tholeiite series
K2O (wt. %)
SiO2 (wt. %)
B
alkalic
alkali-calcic
calc-alkalic
Na2O+K2O (wt. %)
SiO2 (wt. %)
C
metaluminous
peraluminous
peralkaline
molar Al2O3/(Na2O+K2O)
molar Al2O3/(CaO+Na2O+K2O)
D
ferroan
magnesian
FeOt/(FeOt+MgO
SiO2 (wt. %)

Figure

Click here to access/download;Figure;Fig4_Dostal et al_2024_revised.pdf

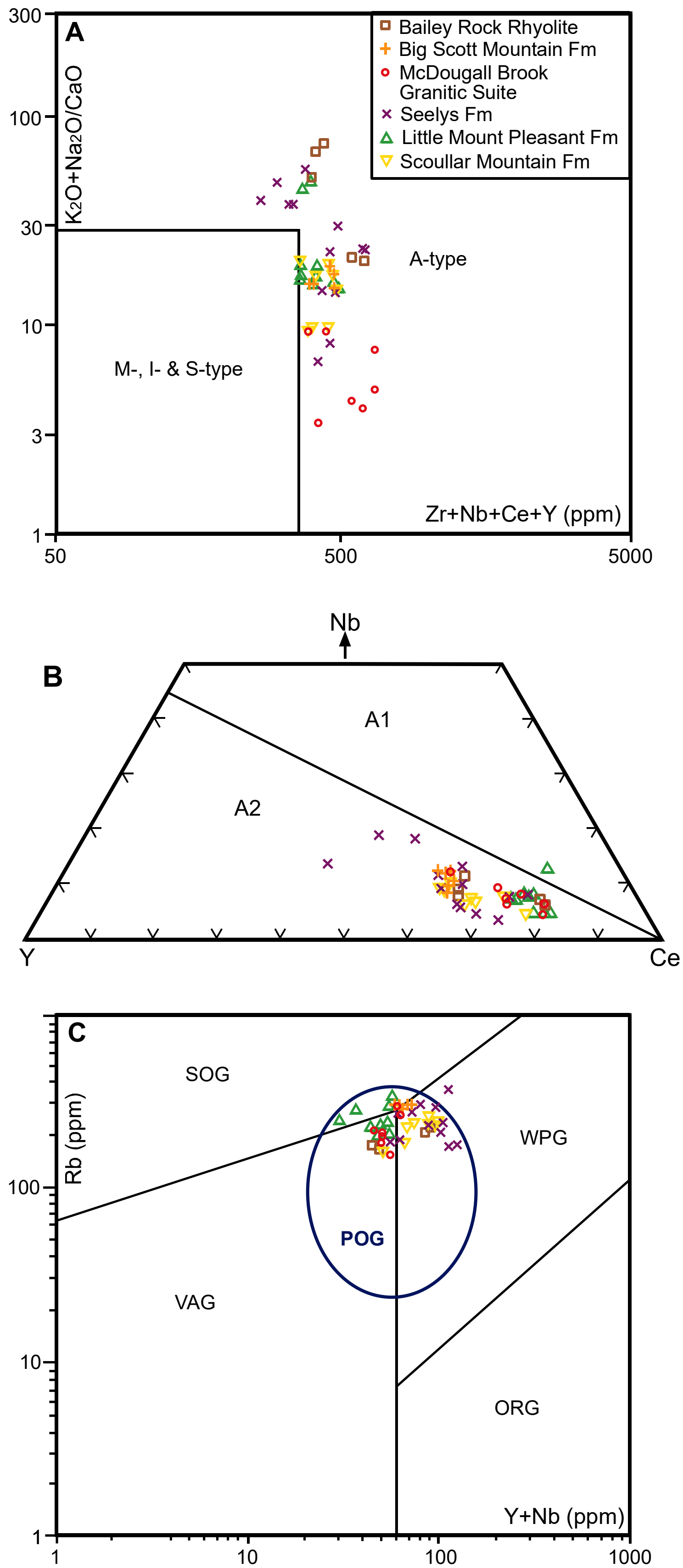

Figure

Click here to access/download;Figure;Fig5_Dostal et al_2024_revised.pdf

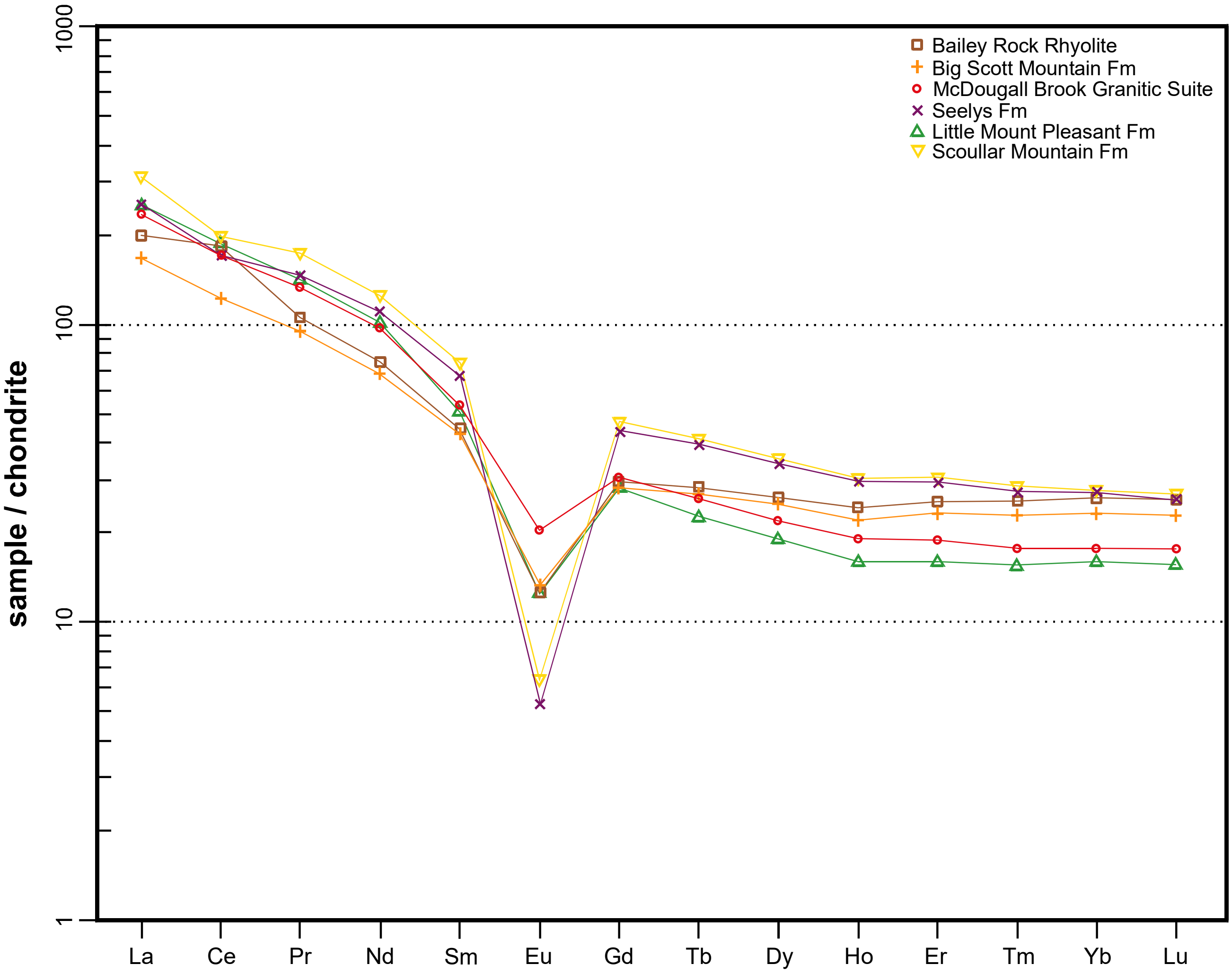

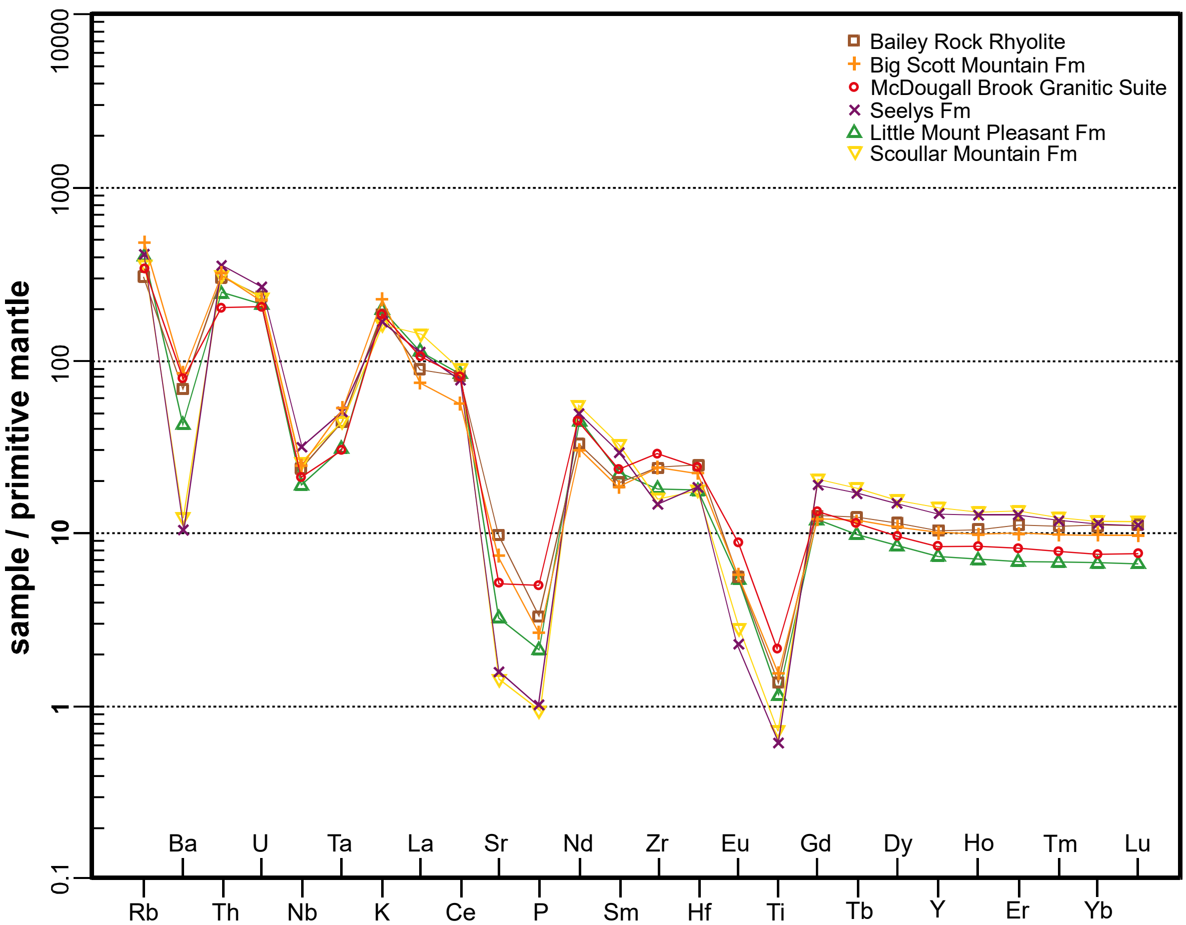
Bailey Rock Rhyolite
Big Scott Mountain Fm
McDougall Brook Granitic Suite
Seelys Fm
Little Mount Pleasant Fm
Scoullar Mountain Fm
sample / primitive mantle
10000
1000
100
10
1
0.1
Rb
Ba
Th
U
Nb
Ta
K
La
Ce
Sr
P
Nd
Sm
Zr
Hf
Eu
Ti
Gd
Tb
Dy
Y
Ho
Er
Tm
Yb
Lu

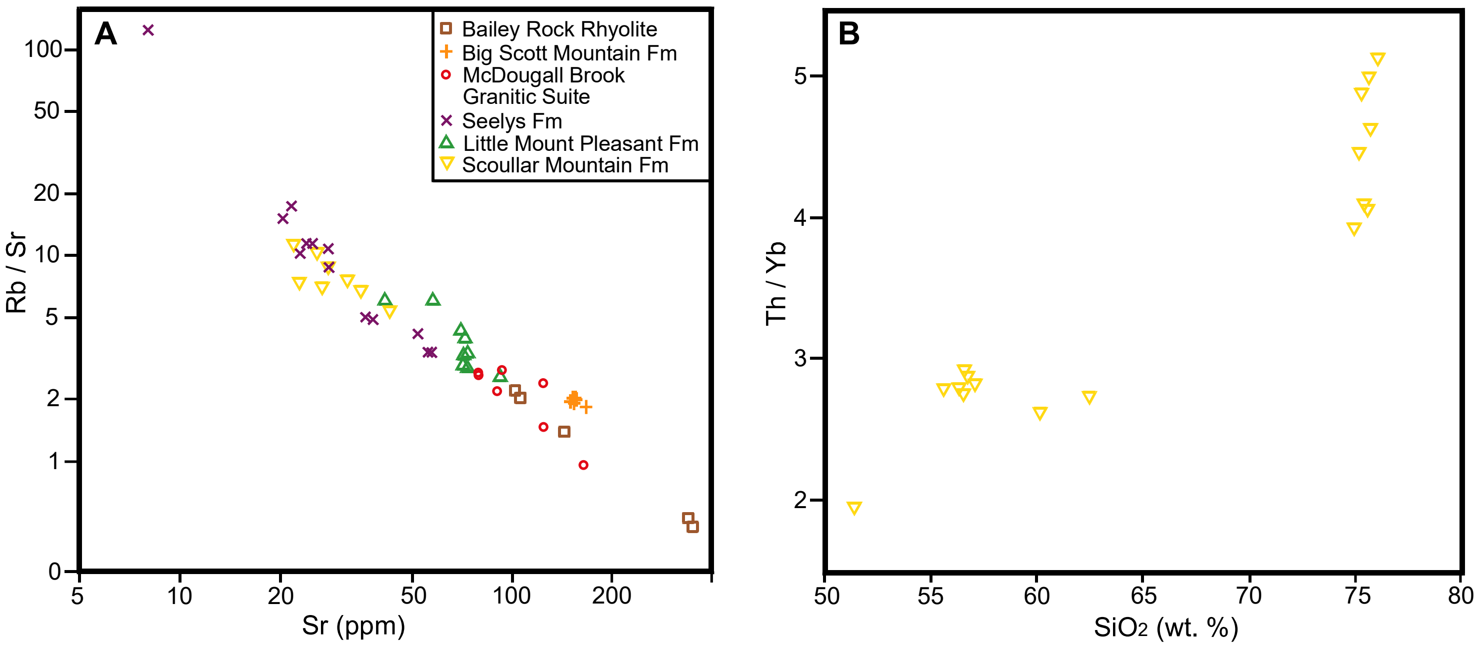
A
Bailey Rock Rhyolite
Big Scott Mountain Fm
McDougall Brook Granitic Suite
Seelys Fm
Little Mount Pleasant Fm
Scoullar Mountain Fm
Rb / Sr
100
50
20
10
5
2
1
0
5
10
20
50
100
200
Sr (ppm)
B
Th / Yb
5
4
3
2
50
55
60
65
70
75
80
SiO2 (wt. %)

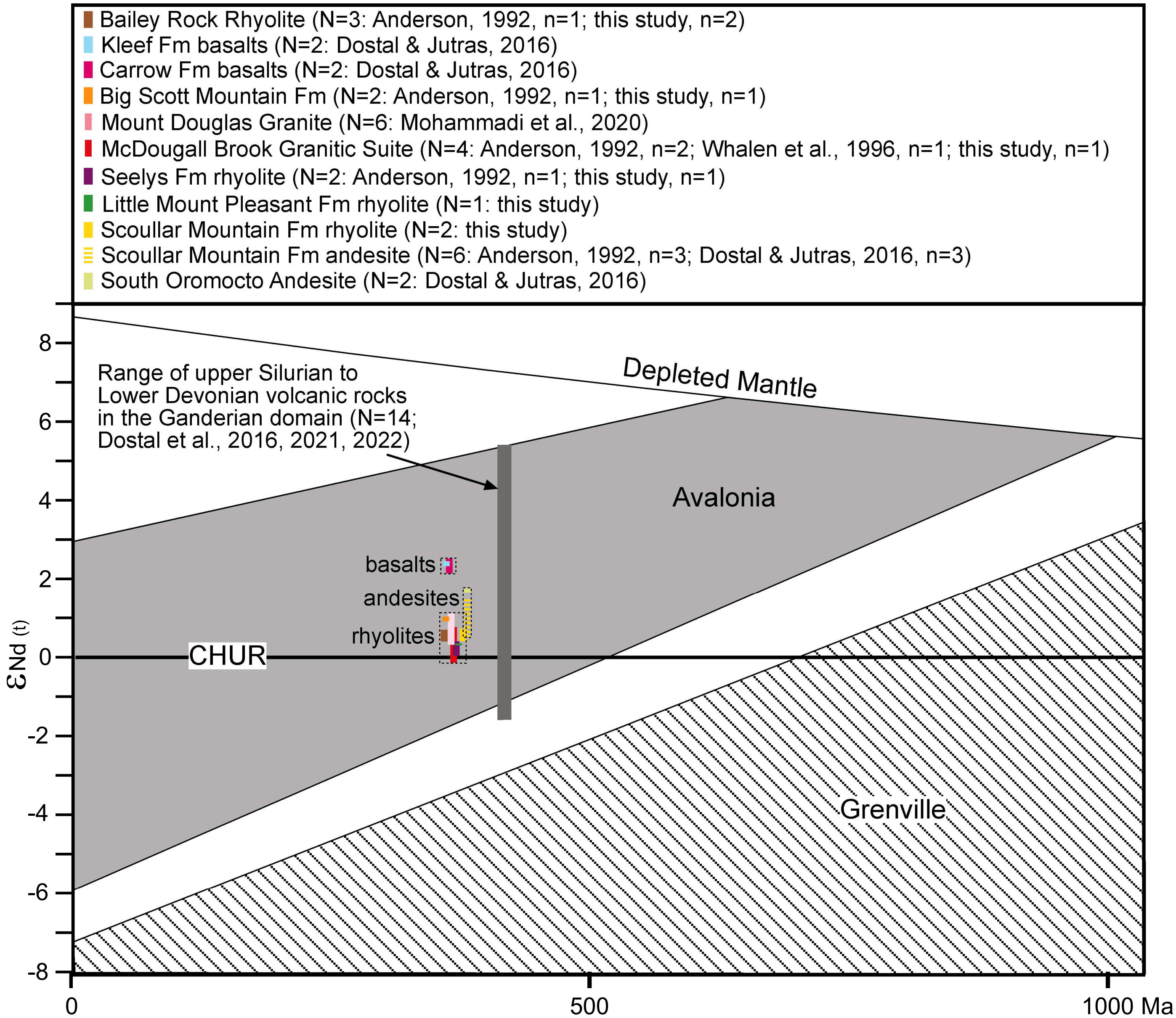
Bailey Rock Rhyolite (N=3: Anderson, 1992, n=1; this study, n=2)
Kleef Fm basalts (N=2: Dostal & Jutras, 2016)
Carrow Fm basalts (N=2: Dostal & Jutras, 2016)
Big Scott Mountain Fm (N=2: Anderson, 1992, n=1; this study, n=1)
Mount Douglas Granite (N=6: Mohammadi et al., 2020)
McDougall Brook Granitic Suite (N=4: Anderson, 1992, n=2; Whalen et al., 1996, n=1; this study, n=1)
Seelys Fm rhyolite (N=2: Anderson, 1992, n=1; this study, n=1)
Little Mount Pleasant Fm rhyolite (N=1: this study)
Scoullar Mountain Fm rhyolite (N=2: this study)
Scoullar Mountain Fm andesite (N=6: Anderson, 1992, n=3; Dostal & Jutras, 2016, n=3)
South Oromocto Andesite (N=2: Dostal & Jutras, 2016)
Range of upper Silurian to Lower Devonian volcanic rocks in the Ganderian domain (N=14; Dostal et al., 2016, 2021, 2022)
Depleted Mantle
Avalonia
basalts
andesites
rhyolites
CHUR
Grenville
εNd (t)
8
6
4
2
0
-2
-4
-6
-8
0
500
1000 Ma

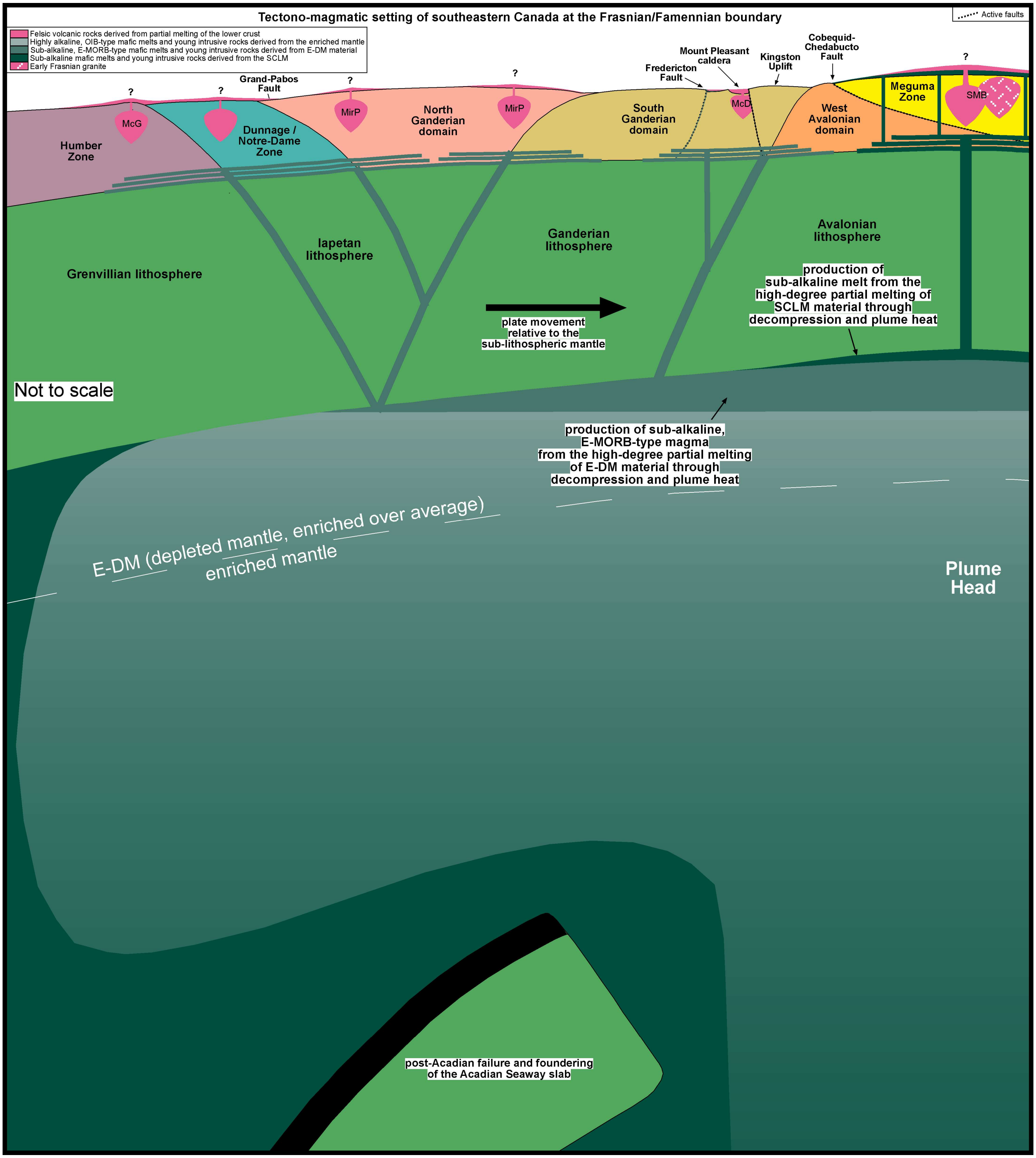
Tectono-magmatic setting of southeastern Canada at the Frasnian/Famennian boundary
Active faults
Felsic volcanic rocks derived from partial melting of the lower crust
Highly alkaline, OIB-type mafic melts and young intrusive rocks derived from the enriched mantle
Sub-alkaline, E-MORB-type mafic melts and young intrusive rocks derived from E-DM material
Sub-alkaline mafic melts and young intrusive rocks derived from the SCLM
Early Frasnian granite
Grand-Pabos Fault
Fredericton Fault
Mount Pleasant caldera
Kingston Uplift
Cobequid-Chedabucto Fault
?
McG
MirP
McD
SMB
Humber Zone
Dunnage / Notre-Dame Zone
North Ganderian domain
South Ganderian domain
West Avalonian domain
Meguma Zone
Grenvillian lithosphere
Iapetan lithosphere
Ganderian lithosphere
Avalonian lithosphere
plate movement relative to the sub-lithospheric mantle
production of sub-alkaline melt from the high-degree partial melting of SCLM material through decompression and plume heat
Not to scale
production of sub-alkaline, E-MORB-type magma from the high-degree partial melting of E-DM material through decompression and plume heat
E-DM (depleted mantle, enriched over average)
enriched mantle
Plume Head
post-Acadian failure and foundering of the Acadian Seaway slab

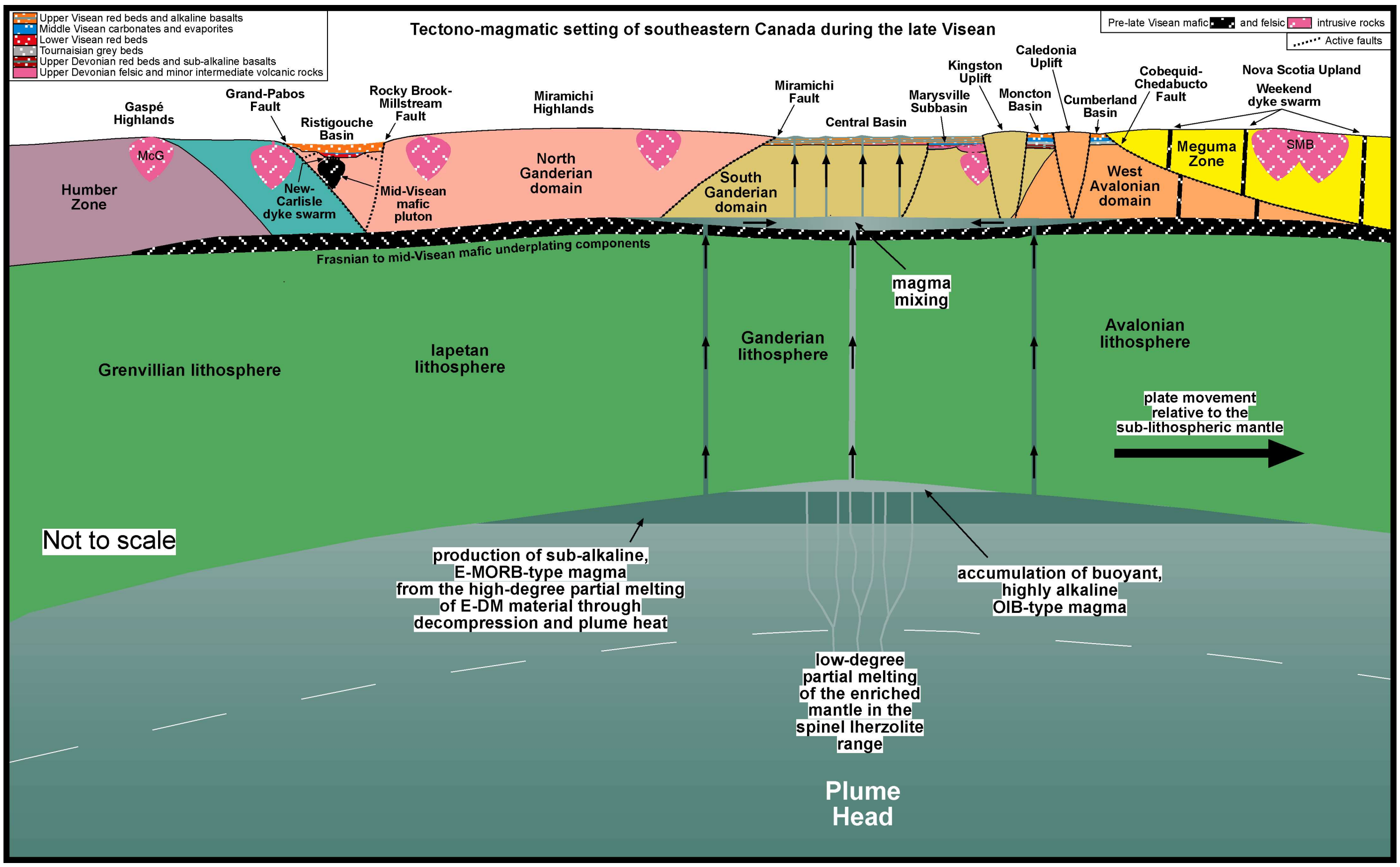
Upper Visean red beds and alkaline basalts
Middle Visean carbonates and evaporites
Lower Visean red beds
Tournaisian grey beds
Upper Devonian red beds and sub-alkaline basalts
Upper Devonian felsic and minor intermediate volcanic rocks
Tectono-magmatic setting of southeastern Canada during the late Visean
Pre-late Visean mafic and felsic intrusive rocks
Active faults
Gaspé Highlands
Grand-Pabos Fault
Ristigouche Basin
Rocky Brook-Millstream Fault
Miramichi Highlands
Miramichi Fault
Central Basin
Marysville Subbasin
Kingston Uplift
Moncton Basin
Caledonia Uplift
Cumberland Basin
Cobequid-Chedabucto Fault
Nova Scotia Upland
Weekend dyke swarm
McG
Humber Zone
New-Carlisle dyke swarm
Mid-Visean mafic pluton
North Ganderian domain
South Ganderian domain
West Avalonian domain
Meguma Zone
SMB
Frasnian to mid-Visean mafic underplating components
magma mixing
Grenvillian lithosphere
Iapetan lithosphere
Ganderian lithosphere
Avalonian lithosphere
plate movement relative to the sub-lithospheric mantle
Not to scale
production of sub-alkaline, E-MORB-type magma from the high-degree partial melting of E-DM material through decompression and plume heat
accumulation of buoyant, highly alkaline OIB-type magma
low-degree partial melting of the enriched mantle in the spinel lherzolite range
Plume Head

Table 1
Major and trace element data.

Sample	SiO_2 wt. %	TiO_2 wt. %	Al_2O_3 wt. %	FeO* wt. %	MnO wt. %	MgO wt. %	CaO wt. %	Na_2O wt. %	K_2O wt. %	P_2O_5 wt. %	LOI wt. %	sum wt. %	V ppm	Pb ppm
Bailey Rock Rhyolite														
22-NB-78	75.92	0.23	11.69	1.65	0.02	0.12	0.12	2.39	5.41	0.07	0.99	98.6	13	14
NB07-39	72.55	0.40	12.73	2.74	0.03	0.26	0.41	2.96	5.51	0.10	1.66	99.4	18	31
NB07-78	75.40	0.22	12.09	1.64	0.02	0.10	0.11	2.41	5.59	0.03	1.04	98.6	16	14
07-NB-39	72.01	0.41	12.92	2.82	0.03	0.30	0.43	3.02	5.39	0.11	2.20	99.7	15	27
07-NB-73	75.81	0.22	11.32	1.92	0.03	0.38	0.15	1.90	5.49	0.05	2.20	99.5	9	21
Big Scott Mountain Formation														
22-32M	74.78	0.37	12.55	1.85	0.03	0.28	0.53	1.53	7.17	0.07	1.25	100.4	16	23
22-33A	75.11	0.30	12.21	2.29	0.04	0.34	0.48	1.38	6.48	0.06	1.40	100.1	6	22
07-32M	74.99	0.37	12.11	1.62	0.03	0.32	0.54	1.55	6.79	0.07	1.10	99.5	16	16
07-33A	74.45	0.30	12.32	2.10	0.03	0.38	0.46	1.53	6.55	0.05	1.50	99.7	13	16
07-32O	73.82	0.33	12.75	2.08	0.03	0.36	0.49	1.53	6.82	0.05	1.42	99.7	14	18
07-33D	73.31	0.35	12.60	2.15	0.03	0.40	0.41	1.44	6.38	0.05	1.63	98.8	17	19
McDougall Brook Granitic Suite														
22-34A	68.96	0.54	13.62	3.70	0.10	0.78	1.72	2.85	5.62	0.14	2.05	100.1	25	15
22-35A	74.90	0.16	11.98	1.48	0.06	0.29	0.81	1.46	6.01	0.01	1.46	98.6	5	32
22-36	68.12	0.59	13.78	3.85	0.10	0.70	1.75	1.14	5.84	0.16	2.87	98.9	27	24
22-37	67.75	0.76	12.82	4.70	0.09	1.43	1.98	0.93	5.81	0.19	3.58	100.0	64	11
07-35A	75.73	0.17	11.80	1.47	0.05	0.33	0.81	1.57	6.02	0.02	1.70	99.7	0	19
07-101	69.53	0.53	13.95	2.89	0.07	0.62	1.06	2.52	5.75	0.14	1.90	99.0	39	71
07-102	69.02	0.51	13.73	2.69	0.07	0.71	1.88	3.11	4.99	0.14	2.10	98.9	27	24
Seelys Formation														
22-44	77.95	0.10	12.19	1.12	0.04	0.13	0.19	2.65	4.87	0.01	0.78	100.0	2	24
22-48	75.03	0.15	12.20	1.65	0.05	0.23	0.52	2.64	5.01	0.02	1.09	98.6	6	14
22-86	76.10	0.16	11.97	1.83	0.05	0.16	0.34	2.59	5.46	0.01	0.73	99.4	2	17
22--88	74.71	0.03	12.88	1.55	0.05	0.02	0.36	3.27	4.90	0.03	0.65	98.4	2	41
07-46	77.01	0.12	11.85	1.29	0.03	0.16	0.14	2.37	5.37	0.02	0.60	99.0	11	33
07-47	77.16	0.11	12.10	1.20	0.03	0.17	0.15	2.22	5.03	0.02	1.20	99.4	13	40
07-50	75.98	0.10	12.28	1.06	0.03	0.13	0.22	3.31	5.03	0.02	1.20	99.4	10	38
07-44	77.30	0.11	11.79	1.10	0.03	0.15	0.20	2.72	4.84	0.02	0.20	98.5	12	16
07-48	75.44	0.16	12.21	1.66	0.05	0.28	0.54	2.73	5.10	0.03	1.20	99.4	10	10
07-81	74.67	0.18	11.93	1.58	0.04	0.34	0.97	2.39	5.46	0.03	1.80	99.4	13	16
07-85	76.25	0.15	11.77	1.42	0.04	0.33	0.26	2.41	5.40	0.02	1.40	99.5	3	19
07-86	75.64	0.17	11.91	1.63	0.04	0.21	0.35	2.62	5.39	0.02	0.90	98.9	10	13
07-84	75.01	0.17	11.58	1.51	0.04	0.31	1.12	2.27	5.31	0.03	1.60	99.0	9	33
Little Mount Pleasant Formation														
22-98	74.82	0.20	12.54	1.32	0.03	0.24	0.49	2.69	5.47	0.02	0.69	98.5	6	25
22-100	74.61	0.22	12.71	1.34	0.04	0.21	0.44	3.01	5.43	0.05	0.71	98.8	7	21
22-106	72.57	0.29	13.21	1.84	0.05	0.31	0.51	1.78	6.98	0.05	1.02	98.6	12	25
07-42	74.27	0.28	13.16	1.64	0.03	0.38	0.17	1.54	6.07	0.05	1.00	98.6	9	23
07-97	75.50	0.22	12.20	1.42	0.04	0.32	0.17	2.14	6.18	0.04	0.80	99.0	0	30
07-104	73.35	0.30	13.04	1.49	0.03	0.25	0.57	2.65	6.23	0.06	1.10	99.1	11	32
07-98	75.35	0.21	12.35	1.29	0.03	0.28	0.51	2.80	5.49	0.04	0.80	99.1	2	17
07-100	75.15	0.23	12.50	1.31	0.03	0.25	0.44	3.01	5.40	0.04	0.80	99.2	11	24
07-106	73.56	0.29	13.15	1.67	0.04	0.35	0.52	1.84	6.81	0.06	1.20	99.5	8	12
Scoullar Mountain Formation														
22--52	75.69	0.14	12.06	1.40	0.04	0.15	0.41	2.99	5.05	0.02	0.46	98.4	2	23
22-53	75.70	0.15	11.91	1.68	0.05	0.24	0.79	2.16	5.36	0.02	1.41	99.5	5	29
22-64	75.31	0.16	12.17	1.98	0.05	0.22	0.88	2.97	5.19	0.02	1.08	100.0	5	27
22-66	74.97	0.16	11.85	1.98	0.07	0.27	0.46	3.16	4.74	0.01	0.77	98.4	7	19
07-48	75.44	0.16	12.21	1.66	0.05	0.28	0.54	2.73	5.10	0.03	1.20	99.4	10	10

Sample	SiO_2 wt. %	TiO_2 wt. %	Al_2O_3 wt. %	FeO* wt. %	MnO wt. %	MgO wt. %	CaO wt. %	Na_2O wt. %	K_2O wt. %	P_2O_5 wt. %	LOI wt. %	sum wt. %	V ppm	Pb ppm
Scoullar Mountain Formation (continued)														
07-52	76.10	0.15	11.90	1.41	0.04	0.19	0.43	3.06	5.12	0.02	0.10	98.5	6	23
07-53	75.18	0.16	12.11	1.47	0.05	0.29	0.80	2.25	5.36	0.03	2.20	99.9	8	20
07-66	75.63	0.17	11.86	1.66	0.07	0.32	0.47	3.15	4.70	0.03	0.90	99.0	5	14

Sample	Zn ppm	Rb ppm	Cs ppm	Ba ppm	Sr ppm	Ga ppm	Ta ppm	Nb ppm	Hf ppm	Zr ppm	Y ppm	Th ppm	U ppm
Bailey Rock Rhyolite													
22-NB-78	15	178	5.90	425	337	18	1.85	12.9	5.40	208	31.8	29.2	4.79
NB07-39	50	214	1.7	532	105	20	1.8	18	8.7	322	66	23.6	5.7
NB07-78	10	168	5.5	438	348	19	2.1	15	6.8	233	33	29.1	4.8
07-NB-39	49	226	2	495	102	20	1.95	21.8	9.3	357	67.7	26.0	5.86
07-NB-73	39	198.5	3.4	538	143	15.4	1.4	17.6	7.7	241	38.6	23.6	3.5
Big Scott Mountain Formation													
22-32M	40	309	18.00	691	167	15	2.15	14.4	5.90	244	44.1	25.3	4.88
22-33A	40	311	17.10	546	154	17	2.34	13.5	5.70	223	48.6	26.5	4.30
07-32M	36	312	20.3	612	155	12	2.14	20.8	7.9	306	45.1	28.5	5.25
07-33A	40	309	19.5	535	152	15	2.24	20.7	7.6	293	49.8	30.0	4.55
07-32O	40	293	16.6	619	153	17	2.1	19	7.3	277	44	26.5	4.6
07-33D	40	291	20.8	528	149	17	2.1	17	7.3	294	45	26.4	4.5
McDougall Brook Granitic Suite													
22-34A	70	156	6.10	731	164	19	1.09	17.3	8.50	460	38.0	13.6	4.22
22-35A	50	213	11.00	127	79	18	1.00	10.3	4.40	160	35.8	19.7	5.21
22-36	60	198	8.50	765	90	18	0.96	12.1	8.10	403	37.8	12.8	3.50
22-37	110	297	14.90	590	124	18	2.08	19.3	7.00	259	42.0	20.6	5.63
07-35A	47	207	11.6	132	79	16	1.32	15.3	6.2	213	34.9	21.9	5.31
07-101	68	260	10.4	793	93	17	1.35	17.1	9.5	425	46.1	17.8	3.68
07-102	64	182.4	9.8	757	124	18.3	1.1	15.9	8.3	348	34.3	15.8	3.3
Seelys Formation													
22-44	30	276	6.80	43	24	17	2.05	16.1	3.50	99	43.3	32.2	5.78
22-48	50	235	5.40	94	23	17	1.64	14.6	4.60	171	72.8	24.4	4.69
22-86	60	180	5.20	95	36	17	1.34	13.6	5.50	180	97.2	21.5	3.77
22--88	70	1000	20.10	21	8	35	15.20	46.5	8.00	114	157.0	44.3	31.10
07-46	33	299.8	5.6	61	27.8	17.3	2.1	27.3	5.6	140	68.2	31.7	5.7
07-47	43	309.5	11.6	45	20.4	18.4	2.3	29.8	5.2	131	48.7	34.7	6
07-50	37	380.1	6.2	33	21.7	19.8	3.4	38.6	6.9	134	72.1	39.5	11.3
07-44	42	287	7.6	63	25	18	2.52	24.5	5.3	137	47	38.3	6.43
07-48	56	247	6	97	28	16	2.24	23.8	6.7	213	79.5	28.4	5.1
07-81	48	193	7.3	124	57	17	1.36	16.7	6.5	230	44.1	21.4	3.85
07-85	45	216	6.2	83	52	15	1.61	17.8	6.1	202	83.1	25.2	4.29
07-86	53	186	5.8	122	38	16	1.36	17.3	6.1	210	104	22.8	3.69
07-84	43	188.5	9.8	86	55.6	16.1	1.2	17.2	6.6	187	37.4	21.1	3.5
Little Mount Pleasant Formation													
22-98	40	231	5.20	145	71	17	1.10	9.5	4.00	150	33.9	21.7	4.95
22-100	30	207	6.50	199	73	17	1.05	9.5	3.30	147	37.7	20.9	3.84
22-106	30	286	6.90	497	72	16	1.09	8.2	4.60	186	27.9	17.8	4.75
07-42	32	249.3	8	387	41.2	16.2	1.2	15.4	6.6	242	14.3	19.0	3.4
07-97	33	349.3	7.2	150	57.5	16.5	1.4	17.4	6.1	173	38	24.0	5.8
07-104	34	235.6	7.3	491	92	16.9	1.2	15.9	7.1	264	32.4	19.2	3.6
07-98	37	244	5.9	145	73	16	1.57	16.2	5.5	198	36.7	25.2	5.4
07-100	36	208	7	195	71	15	1.38	14.4	5.3	201	39.5	22.9	3.99
07-106	37	304	7.2	459	70	16	1.29	14.4	6.6	260	39.4	19.5	4.93

Sample	Zn	Rb	Cs	Ba	Sr	Ga	Ta	Nb	Hf	Zr	Y	Th	U
	ppm	ppm	ppm	ppm	ppm	ppm	ppm	ppm	ppm	ppm	ppm	ppm	ppm
Scoullar Mountain Formation													
22--52	40	169	4.50	52	23	17	1.09	9.7	3.60	134	43.0	21.6	3.40
22-53	50	249	6.20	95	22	16	1.74	16.7	4.80	168	60.2	24.2	4.61
22-64	50	230	5.40	77	43	16	1.71	14.7	4.70	162	56.0	24.2	4.54
22-66	70	243	4.60	106	32	18	2.18	16.1	5.00	140	75.8	27.0	5.55
07-48	56	247	6	97	28	16	2.24	24	6.7	213	80	28.4	5.1
07-52	46	189	5.5	51	27	16	1.59	18	6.6	211	51	26.7	4.04
07-53	46	267	7.3	107	26	17	2.14	24	6.6	213	67	28.1	5.1
07-66	57	236	5	105	35	16	2.14	23	6.4	209	76	27.5	5.31

	La	Ce	Pr	Nd	Sm	Eu	Gd	Tb	Dy	Ho	Er	Tm	Yb	Lu
	ppm	ppm	ppm	ppm	ppm	ppm	ppm	ppm	ppm	ppm	ppm	ppm	ppm	ppm
Bailey Rock Rhyolite														
22-NB-78	27.4	164.00	5.21	17.30	3.41	0.209	2.83	0.65	5.03	1.24	4.14	0.690	5.16	0.8
NB07-39	98.5	150	22.4	77.5	15.1	1.76	13	2	11.8	2.3	6.6	0.96	6.3	0.9
NB07-78	27.5	163	5.43	17.1	3.4	0.24	2.6	0.6	5	1.2	4.3	0.73	5.2	0.8
07-NB-39	106	156	22.3	77.8	15.9	1.95	14.2	2.36	13.4	2.59	7.47	1.07	6.57	0.9
07-NB-73	43.6	96.6	9.48	33.8	5.91	0.44	5.38	1.05	6.6	1.36	4.18	0.64	4.12	0.6
Big Scott Mountain Formation														
22-32M	47.8	94.60	11.30	40.20	8.28	0.916	6.73	1.20	7.47	1.48	4.46	0.664	4.62	0.7
22-33A	57.6	102.00	12.30	41.60	8.23	0.933	7.35	1.23	7.92	1.61	5.03	0.764	4.93	0.7
07-32M	51	101	11.5	42.5	8.59	1.03	7.48	1.33	8.21	1.64	4.89	0.755	4.79	0.7
07-33A	60.6	106	12.8	45	9.05	1.12	8.24	1.5	9.16	1.82	5.39	0.799	5.13	0.7
07-32O	39.5	88.9	10.1	35.1	7.6	0.93	6.9	1.2	7.6	1.5	4.6	0.71	4.9	0.7
07-33D	50.2	101	11.8	40.9	8	0.87	6.9	1.2	7.5	1.5	4.6	0.69	4.7	0.7
McDougall Brook Granitic Suite														
22-34A	61.0	126.00	14.00	53.30	9.77	1.910	7.41	1.14	6.74	1.30	3.84	0.547	3.51	0.6
22-35A	86.7	174.00	19.20	70.80	11.30	0.503	7.56	1.18	6.73	1.32	3.56	0.562	3.71	0.6
22-36	65.6	130.00	15.40	57.70	10.10	1.790	7.44	1.19	6.85	1.33	3.96	0.548	3.90	0.6
22-37	47.2	94.50	10.20	37.40	7.63	1.240	6.70	1.11	6.97	1.45	4.33	0.619	3.87	0.6
07-35A	88.8	178	19.2	62.2	11.5	0.6	8.92	1.31	7.21	1.36	4	0.594	3.75	0.5
07-101	102	161	20.2	71.4	13.2	2.7	11.1	1.63	8.85	1.65	4.66	0.658	4.01	0.6
07-102	67.6	141.4	16	61	9.39	1.75	7.16	1.09	6.09	1.16	3.25	0.5	3.16	0.5
Seelys Formation														
22-44	45.7	104.00	11.90	43.80	9.73	0.188	7.80	1.30	7.95	1.59	4.52	0.663	4.42	0.7
22-48	103.0	166.00	22.10	81.10	15.20	0.454	12.40	1.97	11.90	2.27	6.69	0.999	6.30	1.0
22-86	294.0	296.00	57.60	197.00	30.70	1.180	22.40	3.25	17.50	3.09	7.70	1.000	5.72	0.9
22--88	55.8	139.00	16.50	55.20	14.40	0.020	12.10	2.80	21.00	4.61	16.30	3.080	25.10	4.0
07-46	81.2	138.3	21.51	81.8	16.2	0.28	13.47	2.21	12.86	2.47	7.04	0.99	6.46	0.9
07-47	42.4	85.1	11.89	46.1	9.46	0.22	8.07	1.47	9.13	1.73	5.41	0.79	5.59	0.8
07-50	42.4	95.1	11.4	45	10.1	0.12	10.4	1.98	12.92	2.5	7.49	1.04	6.52	1.0
07-44	52.6	117	13.2	49	11	0.22	9.29	1.61	9.5	1.85	5.5	0.806	5.15	0.7
07-48	107	160	22.1	77.4	15.9	0.62	14.9	2.44	14.1	2.74	7.887	1.14	6.93	1.0
07-81	82.3	159	18	60.5	11.6	0.67	9.66	1.5	8.37	1.6	4.67	0.679	4.3	0.6
07-85	142	186	29	100	19.9	0.68	18.2	2.76	14.8	2.76	7.85	1.14	6.7	0.9
07-86	277	266	51.8	164	29.4	1.3	27	3.55	17.3	3.01	7.97	1.07	6.03	0.8
07-84	77.5	164.1	18.43	71.7	10.9	0.44	8.16	1.24	7.41	1.36	4.07	0.6	4.18	0.6
Little Mount Pleasant Formation														
22-98	82.5	168.00	18.60	63.50	10.70	0.625	7.21	1.07	6.35	1.22	3.35	0.486	3.35	0.5
22-100	90.0	165.00	19.70	69.80	10.60	0.822	7.82	1.20	6.59	1.12	3.59	0.515	3.41	0.5
22-106	74.6	147.00	16.50	58.80	9.40	1.210	6.27	0.93	5.48	1.03	2.99	0.460	2.93	0.5
07-42	36.5	93.7	8.88	31.3	4.58	0.55	3.2	0.47	2.78	0.56	1.58	0.27	1.95	0.3
07-97	97.8	160.2	22.35	83.4	11.6	0.69	8.16	1.2	7.15	1.21	3.48	0.55	3.69	0.5
07-104	76.4	151.4	17.91	64.4	9.81	1.3	7.03	1.07	6.36	1.19	3.33	0.5	3.54	0.5

	La ppm	Ce ppm	Pr ppm	Nd ppm	Sm ppm	Eu ppm	Gd ppm	Tb ppm	Dy ppm	Ho ppm	Er ppm	Tm ppm	Yb ppm	Lu ppm
Little Mount Pleasant Formation (continued)														
07-98	82.7	162	18	58.9	11.2	0.71	8.71	1.27	6.95	1.34	3.91	0.578	3.61	0.5
07-100	86.4	150	18.5	61.8	11.2	0.93	9.15	1.36	7.6	1.46	4.23	0.617	3.85	0.6
07-106	75.5	144	15.7	52.6	9.84	1.39	7.5	1.07	5.78	1.11	3.3	0.504	3.27	0.5
Scoullar Mountain Formation														
22--52	85.5	171.00	19.00	68.80	11.90	0.295	8.44	1.33	7.79	1.51	4.50	0.614	4.32	0.7
22-53	99.5	151.00	21.70	77.90	13.90	0.489	11.20	1.82	11.00	2.08	5.86	0.850	5.22	0.8
22-64	76.5	146.00	18.00	64.50	12.40	0.348	9.72	1.61	9.62	1.89	5.44	0.782	4.95	0.8
22-66	118.0	179.00	25.80	95.60	17.50	0.524	14.20	2.32	13.60	2.64	7.34	1.060	6.86	1.0
07-48	107	160	22.1	77.4	15.9	0.62	14.9	2.44	14.1	2.74	7.89	1.14	6.93	1.0
07-52	89.9	172	19.8	65.8	13	0.37	10.9	1.72	9.93	1.95	5.75	0.84	5.2	0.7
07-53	101	147	21.6	73.6	14.9	0.55	13.4	2.12	11.9	2.29	6.72	1	6.29	0.9
07-66	109	157	22.9	80.2	16.7	0.58	15.1	2.41	13.4	2.52	7.4	1.09	6.76	1.0

Table 2

Nd isotopic composition of Piskahegan Group rhyolites and associated granite.

Unit	Sample	Age (t) (Ma)	Nd(ppm)	Sm(ppm)	$^{147}Sm/^{144}Nd$	$^{143}Nd/^{144}Nd(m)$	2σ	$^{143}Nd/^{144}Nd(i)$	$\varepsilon_{Nd}(t)$	T_{DM} (Ma)
Bailey Rock Rhyolite	NB07-39	363.4+/-1.8	75.1	14.1	0.1135	0.512476	7	0.512206	0.70	869
Bailey Rock Rhyolite	NB07-73	363.4+/-1.8	29.4	5.48	0.1127	0.512462	7	0.512194	0.47	883
Big Scott Mountain Fm	NB07-32O	364.6+/-0.7	33.39	7.06	0.1278	0.512522	7	0.512217	0.95	930
McDougall Brook Granite Suite	NB07-35A	370+/-2	70.8	11.3	0.0966	0.512417	6	0.512183	0.42	822
Seelys Fm	NB07-88	372?	51.28	13.35	0.1574	0.512566	7	0.512184	0.46	1286
Little Mount Pleasant Fm	NB07-98	373?	66.52	10.62	0.0965	0.51241	7	0.512174	0.33	830
Scoullar Mountain Fm	NB07-53	374.6+/-0.9	77.9	13.9	0.108	0.512444	6	0.512179	0.46	870
Scoullar Mountain Fm	NB07-66	374.6+/-0.9	95.6	17.5	0.1107	0.512463	8	0.512191	0.70	865

Notes: the approxinate age of undated units, marked with a question mark, is based on stratigraphic constraints; $^{143}Nd/^{144}Nd(m)$ = measured value; $^{143}Nd/^{144}Nd(i)$ = initial, calculated value; $\varepsilon_{Nd}(t)$ = age-corrected values for the crystallization age (t); T_{DM}-depleted mantle model age calculated using the model of DePaolo (1988).

Table 3. Saturation temperatures.

Unit:		Zircon T_{Zr} (°C) W & H (1983)		Boehnke et al. (2013)		Monazite T_{Mz} (°C) Montel (1993)		Apatite T_{Ap} (°C) H & W (1984)	
	n	average	sd	average	sd	average	sd	average	sd
Big Scott Mountain Fm	6	851	12	824	15	848	13	894	19
Bailey Rock Rhyolite	5	848	15	820	16	865	17	906	33
Seelys Fm	13	800	19	762	22	892	44	821	22
Little Mount Pleasant Fm	9	818	22	783	28	878	11	869	23
Scoullar Mountain Fm	8	804	18	764	22	882	14	820	27
McDougall Brook Granitic Suite	7	851	30	819	35	859	35	892	69

n-number of samples; sd-standard deviation; W-Watson; H-Harrison